COO-3130TB-253

PROGRESS REPORT OF A RESEARCH PROGRAM

IN EXPERIMENTAL HIGH ENERGY PHYSICS

Progress Report
for Period January 1, 1979 - December 31, 1979

Anatole M. Shapiro

Brown University
Providence, Rhode Island

October 1, 1979

PREPARED FOR THE U. S. DEPARTMENT OF ENERGY UNDER CONTRACT EY-76-C-02-3130.A003
(TASK B-EXPERIMENTAL)

DISCLAIMER

NOTICE

ABSTRACT

An experimental program in strong and electromagnetic interaction physics of elementary particles is being carried out using three hybrid bubble chamber systems. Experiments are being performed utilizing the accelerators of the laboratories at Batavia, Stanford, and Geneva, Switzerland.

The bubble chamber - hybrid system group is engaged in several experiments at the Fermilab. Extensive analysis of multiparticle production in $\pi^- p$ interactions at 147 GeV/c has been carried out, with particular emphasis this year on a comparison of our data with electroproduction data of hadrons with high-p_T and with the Field and Feynman quark-quark scattering model. Preliminary results have also been presented on an investigation of $\pi^+ p$, $K^+ p$, and pp interactions at the same momentum; and this work is continuing. Two much higher statistics experiments will start later in 1980 at FNAL to study $\pi^\pm$, K^+, and $p^\pm$ interactions in hydrogen, and in aluminum, silver, and gold foils, at beam momenta of 200 and 400 GeV/c. A similar study of $\pi^+ p$, $K^+ p$, and pp interactions at 250 to 300 GeV/c using the large European Hybrid System at CERN will also be started. In addition, we shall begin an experiment on charm and vector meson photoproduction in a polarized monoenergetic backscattered laser beam of 20 GeV using the SLAC Hybrid Facility.

Progress Report of a Research Program in Experimental High Energy Physics

The Department of Physics at Brown University presents herein a report of the progress made in the experimental program during the present contract period (1 January 1979 - 31 December 1979). This work has been supported by the U. S. Department of Energy under Contract EY-76-C-02-3130.A003 (Task B-Experimental).

This report on the bubble chamber-proportional hybrid system program is divided as follows:

I. Data Analysis in Progress

II. Experimental Runs in Progress and in Preparation

III. Associated Matters

IV. Scientific Personnel

V. Papers Published During the Preceding Year and Papers in Press

I. Data Analysis in Progress.

(a) Studies of $\pi^+ p$, $K^+ p$ and pp Interactions at 147 GeV/c (FNAL Experiment 299) and of $\pi^- p$ Interactions at 147 GeV/c (FNAL Experiment 154) using the Proportional Wire Chamber-Bubble Chamber Hybrid System at Fermilab.

These two experiments are complementary studies of the characteristics of high energy interactions as a function of the quantum numbers of the four incident projectile particles.

Experiment 154 is essentially completed, with just a few remaining papers in the process of being published. Four papers appeared during the past year in Physical Review D and in Nuclear Physics B, and three more are in press. However, the data from E-154 are being used more and more in comparisons with the data from E-299.

The data of E-299 were obtained from two exposures of the Fermilab Proportional Wire Chamber - 30 inch Bubble Chamber Hybrid System (PHS) in tagged beams of positive particles of 147 GeV/c momentum. The portion of the hybrid system upstream of the bubble chamber provides for the identification of incoming particles by Cerenkov counters, and for the precise determination of their direction and momentum by proportional wire counters. Proportional wire chambers in the downstream portion of the hybrid system provide precise measurement of the momentum and direction of fast forward-going charged particles emerging through the fringing field of the bubble-chamber magnet. The bubble chamber itself serves as the target and provides 4π sensitivity for all charged particles produced in any interaction in the chamber and considerable detection efficiency for associated V^o's and γ's

as well. The linking of the electronic data with the tracks in the bubble chamber allows us to use the upstream Cerenkov signal to identify each interacting beam particle, so that we obtain data simultaneously for all the kinds of particles present in the beam, and can make comparisons with a minimum of systematic errors.

The first 158,000 frames were obtained in a beam of positive particles divided approximately equally between π^+ mesons and protons, with only a small percentage of K^+. An enrichment of the K^+ component of the beam to about 10 percent was achieved for the second positive beam run, consisting of 240,000 pictures, and this second run was further enhanced by the use of a prototype of the forward gamma detector planned for future exposures. This prototype is full scale except in area perpendicular to the beam, which is 30 cm x 30 cm rather than the final 75 cm x 75 cm. These prototype data allow us to analyze the forward-going electromagnetic radiation produced in the observed interactions, within the small solid angle subtended.

All of the film has been scanned and predigitized, and precision measurements have been completed on nearly all of the pictures.

Results obtained thus far in this experiment, together with some comparisons with our π^-p experiment, have been presented in contributed papers (see Section V, References 307-314 and 316-318) and in papers in press (References 319-322). The reports on E-299 data represent preliminary analyses of the available data and work on all areas is continuing. Some of this work is described briefly below.

(i) Comparison of Hadronic Production in $\pi^- p$ Interactions and also $\pi^+ p$, $K^+ p$, and pp Interactions with Hadronic Production by Leptons.

One of the most exciting developments during the past year has been the comparison of our multiparticle events with the jet production in $e^- p$ experiments and other lepton experiments. The jet production in the lepton studies is all at high transverse momentum and is interpreted as the hard scattering of a virtual photon from the lepton by a quark in the proton, as in Figure 1(a). There are a number of quark-parton models that make predictions for leptoproduction of hadrons, as well as for hadron production of hadrons, all at large transverse momenta.[1-5] We have observed that our events, essentially all with very small transverse momenta, have similar properties.

We have compared our data particularly with a study[6] of the electroproduction of charged hadrons ($e^- + p \rightarrow e^- +$ hadrons), performed at Cornell, and with curves from the Field and Feynman quark model[1] predicting the distributions of the fastest and second fastest charged hadrons with respect to the variable z. For electroproduction, this variable is defined to be $z = P_{lab}/\nu$, where P_{lab} is the laboratory momentum of the hadron and ν is the laboratory energy of the virtual photon (see Fig. 1(a)); whereas for hadron production, we define $z = (E^* + P_{\parallel}^*)/\sqrt{s}$, where E^* and $P_{\parallel}^*$ are the energy and longitudinal momentum of the hadron in the center-of-mass system and $\sqrt{s}$ is the center-of-mass energy.[1] The variable z is familiar from electroproduction studies and, although it is not commonly used to

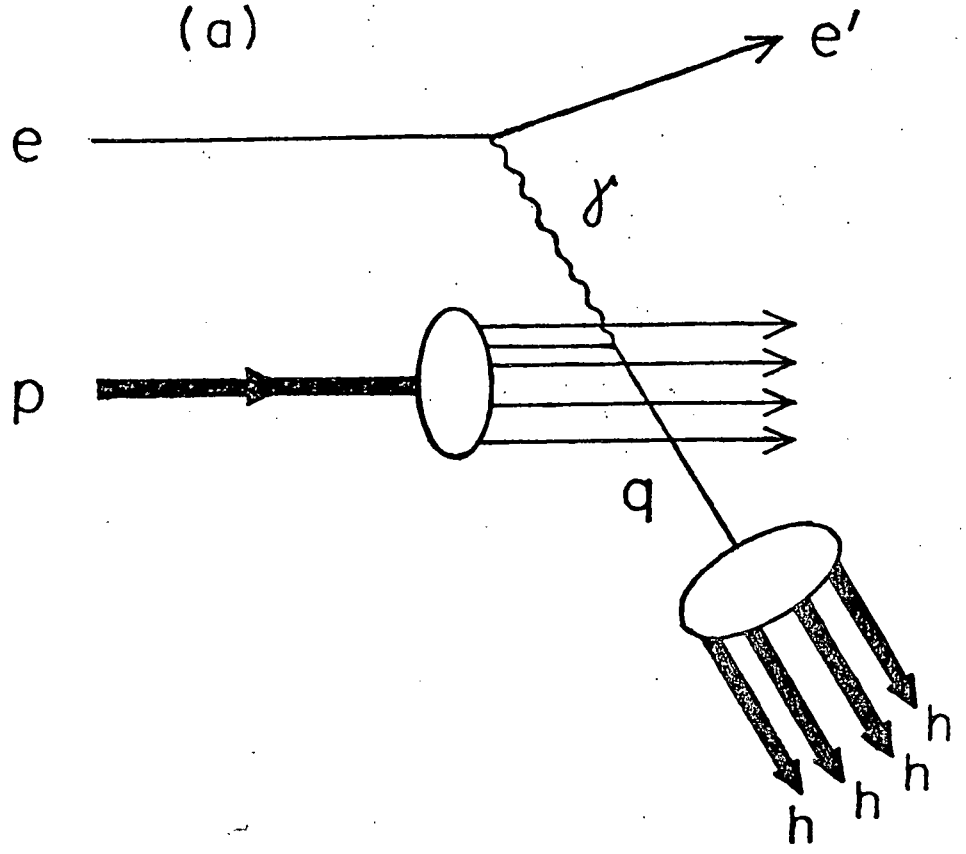

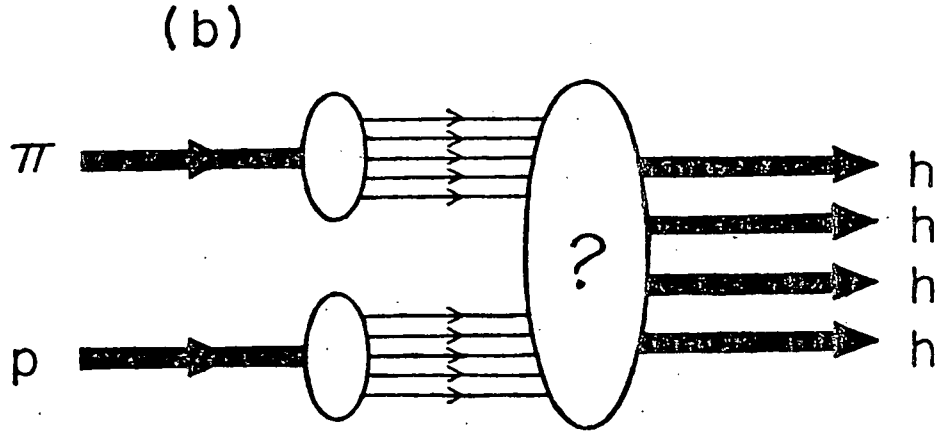

Fig. 1

describe hadron data, we have chosen it to facilitate comparison with the electroproduction data and thereby directly exhibit the striking similarity between these two very different types of reactions.

Figure 1(a) pictures the generally accepted mechanism for deep-inelastic electroproduction as described by the quark-parton model. The incident electron emits a virtual photon γ with invariant mass $-Q^2$ and laboratory energy ν. This virtual photon is assumed to be absorbed by a single quark (or anti-quark) which is then ejected from the original proton and subsequently breaks up into a hadron jet whose final hadrons have invariant mass W. At sufficiently high Q^2 and W, this quark breakup can be described by the quark fragmentation function $D_q^h(z)$, which is the probability of a hadron of type h arising from the fragmentation of the quark q having momentum fraction $z = P_{lab}/\nu$.

Figure 1(b) depicts the production of hadrons at small transverse momentum by pions incident on protons in terms of the quark-parton model, indicating the theoretical uncertainty concerning this process. In this picture, the quarks in both the pion and the proton interact in an as yet unknown way and produce the final state hadrons. In this study, we compare the large transverse momentum process of Fig. 1(a) with the small transverse momentum process of Fig. 1(b).

In order to compare their data with the models in Refs. (1-5), the authors in Ref. (6) removed elastic ρ production from their sample. In order to permit comparison of our data with theirs, we therefore eliminated both elastic scattering and most of the diffractive events from our sample.

This was done by removing all events that had no or only one charged particle in the forward hemisphere in the center-of-mass. This cut effectively eliminated all two-charged-prong events and some events from other topologies. Finally, in order to check the possible influence of remaining diffractive events on our data, we studied the effect of removing the four-charged-prong events from the sample since they contain most of the remaining diffractive events.

Figure 2(a) directly compares our data with the electroproduction data of Ref. (6) and the theoretical curves of Ref. (1). The z distributions are shown for the two different experiments for the fastest (largest z) charged particle in each event and for the second fastest (next largest z) charged particle. The solid and dashed curves are the Field-Feynman predictions for these distributions. Within the experimental errors, the agreement of our data with both the electroproduction and the Field-Feynman model is quite good except at z near 1. If one compares this figure with Fig. 2(c), which gives the results for data with the four-charged-prong events removed, it can be seen that the agreement improves. This probably reflects the effect of the remaining diffractive events that tend to be concentrated in the four-charged-prong events. In Fig. 2(b) we present the comparison of our data with the curves from the Field Feynman model for the distributions of the fastest positive and fastest negative charged particles from deep-inelastic electroproduction. Again, the agreement is surprisingly good, and it is even better when the four-charged-prong events have been removed (not shown).

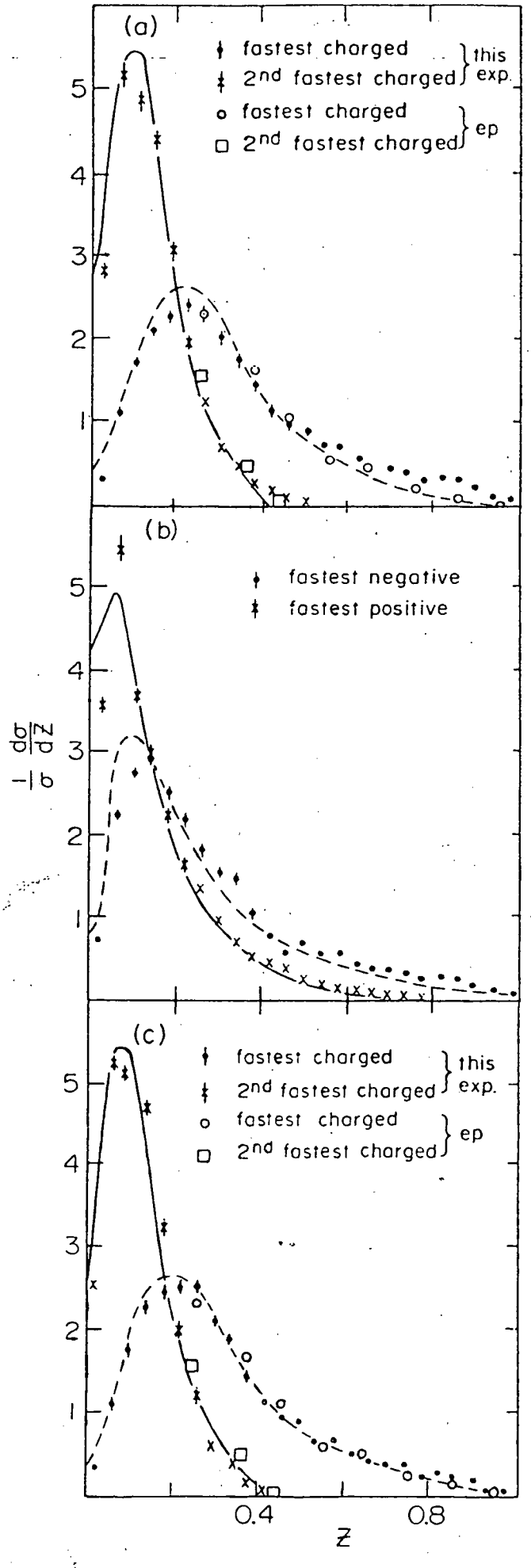
(a)
fastest charged
2nd fastest charged
this exp.
fastest charged
2nd fastest charged
ep
(b)
fastest negative
fastest positive
(c)
fastest charged
2nd fastest charged
this exp.
fastest charged
2nd fastest charged
ep
1/σ dσ/dz
z
0.4
0.8

Fig. 2

In Figure 2, $\frac{1}{\sigma}\ \frac{d\sigma}{dz}$ is plotted without any scale factors and the curves have not been fit to the data. We note that the above model was developed with large transverse momentum jets in mind and was explicitly not intended to apply to low transverse momentum data such as those in our experiment. In light of this point and since the kinematics of Fig. 1(a) are very different from the kinematics of Fig. 1(b), it is surprising that the results of this experiment and the experiment described in Ref. (1) are so similar. Other authors have pointed out similarities between low and high momentum transfer processes,[7] and similarities between hadron- and lepton-produced final states have also been noted.[8] To our knowledge, this is the first comparison of the two processes shown in Fig. (1) with respect to the variable z.

The above comparison using the π^-p data from E-154 has been submitted to the Phys. Rev. Letters for publication (Sec. V, Ref. 319), and we are vigorously continuing this comparison with the data from E-299 as it nears completion. To date, the z distributions for the π^+p, K^+p, and pp events are in very good agreement with the data and curves in Figure 2.

REFERENCES

1. R. D. Field and R. P. Feynman, Nucl. Phys. B136, 1 (1978).

2. L. M. Sehgal, Proceedings of the 1977 International Symposium on Lepton and Photon Interactions at High Energies, Hamburg, Germany, 1977, edited by F. Gutbrod (Deutsches Elektronen Synchrotron).

3. B. Andersson, G. Gustafson, and C. Peterson, Nucl. Phys. B135, 273 (1978).

4. R. D. Field and R. P. Feynman, Phys. Rev. D15, 2590 (1977).

5. R. P. Feynman, R. D. Field, and G. C. Fox, Nucl. Phys. B128, 1 (1977).

6. G. Drews et al., Phys. Rev. Lett. 41, 1433 (1978).

7. W. Ochs, Nucl. Phys. B118, 397 (1977), and references therein.

8. C. del Papa et al., Phys. Rev. D15, 2425 (1977);
M. Derrick et al., Phys. Rev. D17, 1 (1978);
H. Rudnicka et al., "Characteristics of Hadrons Produced in ν_μNe and $\bar{\nu}_\mu$Ne Interactions," presented at the Neutrino '78 Conference at Purdue University, April 28, 1978.

(ii) Inclusive Production of Neutral Strange Particles in π^+p, K^+p, and pp Interactions at 147 GeV/c.

At high energies, neutral strange particle production has been studied in pp collisions at 100 GeV/c,[1,2] 200 GeV/c,[3,4] 300 GeV/c,[5,6] and 400 GeV/c.[7] However, there is only one such study in π^+ collisions[1] and none in K^+p. This experiment represents the first attempt to measure inclusive production at Fermilab energies for all three types of beam particles in the same experiment.

The interactions studied in our experiment are listed in Table I, together with the inclusive cross sections found. To calculate these cross sections, each V^o which was found and identified as a strange particle was weighted to account for scan inefficiency, measurement and geometry reconstruction losses, detection inefficiency due to the imposition of a minimum-length cut and decay-volume restriction, and neutral decay modes. However, no correction was made for the contribution from K_L, and no attempt was made to resolve the Λ-Σ° ambiguity. The average weight was 3.4 for K_s, and 3.3 for Λ. (The quoted errors include estimates of the uncertainty in each of the corrections made, and the uncertainty in the procedure for resolving ambiguities, in addition to the statistical error.)

These total inclusive cross sections can be compared with data of experiments at other energies, mostly studies of pp interactions.

For K_s° production, reactions (1)-(3), our result for pp is in excellent agreement with the rising trend exhibited by the other pp experiments in the

TABLE I: Total Inclusive Cross Sections

	Reaction	Inclusive Cross Section (mb)
(1)	$\pi^+ p \to K_s$ + anything	4.0 ± 0.3
(2)	$K^+ p \to K_s$ + anything	5.9 ± 1.0
(3)	$pp \to K_s$ + anything	5.0 ± 0.2
(4)	$\pi^+ p \to \Lambda$ + anything	1.8 ± 0.2
(5)	$K^+ p \to \Lambda$ + anything	1.4 ± 0.4
(6)	$pp \to \Lambda$ + anything	4.2 ± 0.2
(7)	$\pi^+ p \to \bar{\Lambda}$ + anything	0.7 ± 0.1
(8)	$K^+ p \to \bar{\Lambda}$ + anything	0.5 ± 0.2
(9)	$pp \to \bar{\Lambda}$ + anything	0.8 ± 0.2

laboratory momentum range of 70-300 GeV/c. Our K_s cross section for π^+p agrees with an experiment[1] at 100 GeV/c which is the only measurement above 25 GeV/c. Data for K_s production in K^+p is only available up to 32 GeV/c; they show much larger values for the cross section than for π^+p or pp, but a gentler energy dependence. Our value at 147 GeV/c for $K^+p \rightarrow K_s^\circ$ is comparable to the pp cross section, but the errors do not yet permit a meaningful quantitative comparison. Furthermore, there are systematic problems involved in detecting the fast-forward K° decays from diffractive beam dissociation. It is unlikely that the entire K_s cross section from K^+ has been measured.

For inclusive Λ production, reactions (4)-(6), the pp data appear to level off about 70 GeV/c, a pattern that is confirmed by our experiment. Our value for π^+p is consistent with that for π^-p in this energy range. The K^+p results at lower energies indicate a rapidly rising cross section with energy. From 8 to 32 GeV/c the cross section rises by a factor of three. Our value at 147 GeV/c is about twice as large as the one at 32 GeV/c.

For inclusive $\bar{\Lambda}$ production, reactions (7)-(9), the errors in all experiments are large, but it is apparent that all the cross sections are rising sharply. Furthermore, the inclusive $\bar{\Lambda}$ cross section appears to be around half the inclusive $\bar{p}$ production rate for pp collisions at energies above 50 GeV/c.[8] This result is in agreement with various constituent model predictions of strange-quark pair production relative to non-strange production.[9] Our results are in agreement with this trend.

Tables II and III give the topological cross sections by beam type for inclusive K_s and Λ production, respectively. Figures 1(a) and (b) show the average number of K_s and Λ per collision, respectively, as a function of topology for reactions (1)-(4) and (6). In the cases of reactions (4) and (6), only those lambdas produced in the backward hemisphere in the center-of-mass system are included in Figure 1(b). The lines shown represent the best linear fits to the data. For reaction (2) the point at $n_{ch}=2$ has been omitted from the fit because of the loss of fast, forward, diffractively produced K_s. The slopes of all the fitted lines are consistent with zero; however, only the fits to Λ production yield reasonable χ^2, as shown. Therefore, it can be concluded that, within the experimental errors, Λ production is independent of charged particle multiplicity. This agrees with the hypothesis that Λ's result primarily from target fragmentation while most of the charged particles are produced in the central region.

Although the slopes of the best linear fits to the K_s data are also consistent with zero, the chi-squared values are generally poorer, and it is more difficult to draw any conclusions about the nature of the dependence, if any, of $\langle K_s^\circ \rangle_n$ on the number of charged particles n.

The average number of Λ's produced per inelastic collision in the backward hemisphere is the same, within experimental errors, for reactions (4) and (6), 0.06 ± 0.01 and 0.07 ± 0.01, respectively. This is consistent with the result in Figure 1, since target fragmentation should proceed in the same manner, regardless of beam type. However, the average number of

TABLE II: Topological Cross Sections σ_n for K°_s Production

	σ_n(mb)		
	Beam Particle		
Multiplicity n	π^+ (Reaction 1)	K^+ † (Reaction 2)	p (Reaction 3)
2	0.16 ± 0.06	0.04 ± 0.04	0.30 ± 0.07
4	0.68 ± 0.18	0.92 ± 0.34	0.66 ± 0.11
6	0.85 ± 0.15	0.56 ± 0.18	1.28 ± 0.19
8	0.92 ± 0.12	0.54 ± 0.17	0.96 ± 0.12
10	0.72 ± 0.09	0.88 ± 0.27	0.63 ± 0.10
12	0.45 ± 0.07	0.41 ± 0.15	0.55 ± 0.09
14	0.24 ± 0.07	0.04 ± 0.04	0.12 ± 0.04
16	0.02 ± 0.02	0.05 ± 0.05	0.06 ± 0.03
18	0.04 ± 0.02	---	0.01 ± 0.01
20	0.01 ± 0.01	0.06 ± 0.06	0.02 ± 0.02

†In the K^+ beam sample, K°_s events with rapidity >1.5 have been eliminated.

TABLE III: Topological Cross Sections σ_n for Λ Production

(backward hemisphere only)

Multiplicity n	σ_n(mb) Beam Particle π^+ (Reaction 4)	σ_n(mb) Beam Particle p (Reaction 6)
2	0.11 ± 0.04	0.18 ± 0.05
4	0.15 ± 0.04	0.44 ± 0.07
6	0.27 ± 0.05	0.41 ± 0.08
8	0.34 ± 0.06	0.52 ± 0.09
10	0.14 ± 0.03	0.31 ± 0.07
12	0.10 ± 0.03	0.13 ± 0.05
14	0.03 ± 0.02	0.08 ± 0.03
16	0.04 ± 0.02	0.04 ± 0.02
18	0.01 ± 0.01	---

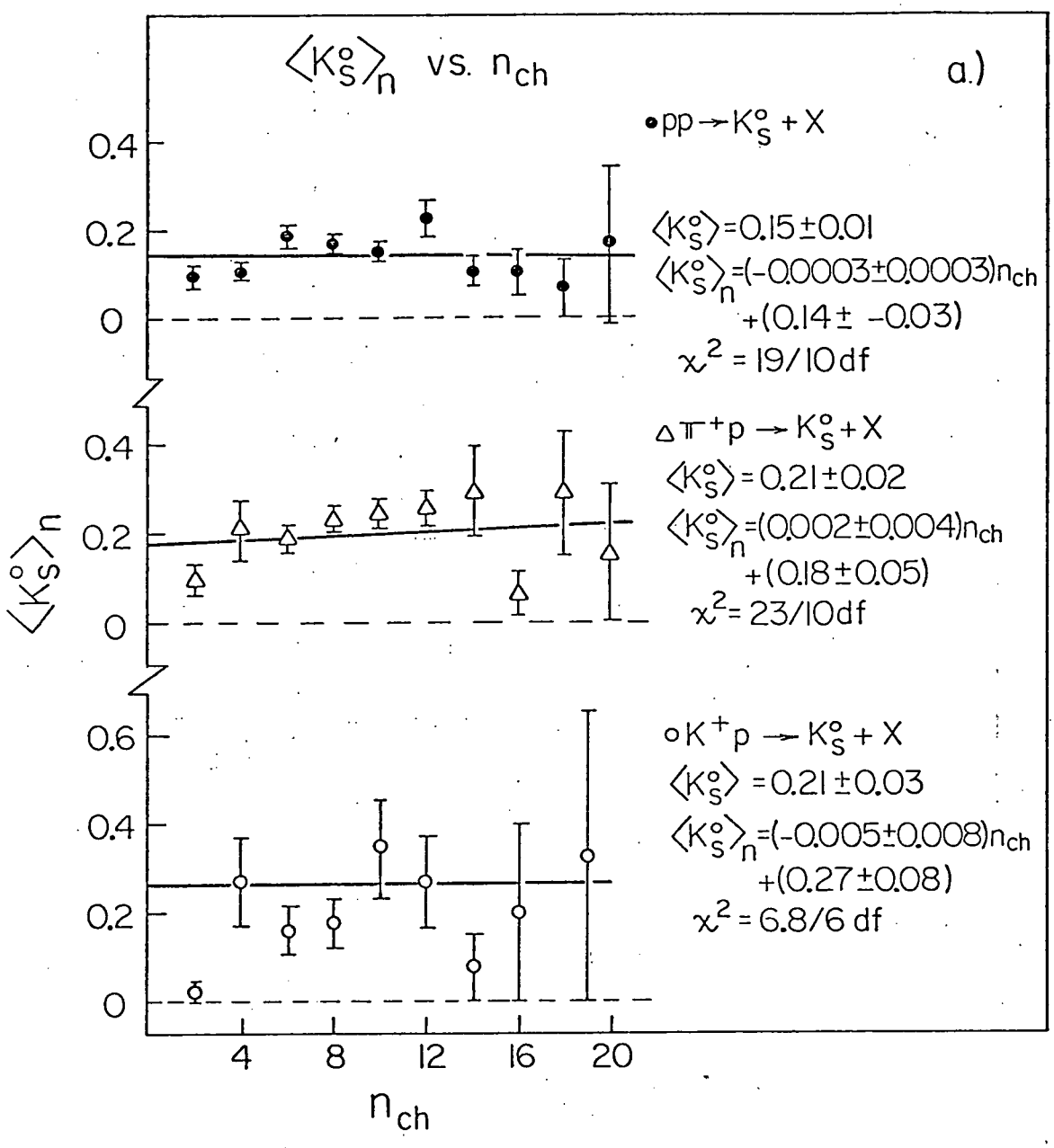
$\langle K^0_S \rangle_n$ vs. n_{ch}
a.)
• $pp \to K^0_S + X$
$\langle K^0_S \rangle = 0.15 \pm 0.01$
$\langle K^0_S \rangle_n = (-0.0003 \pm 0.0003) n_{ch} + (0.14 \pm -0.03)$
$\chi^2 = 19/10$ df
$\Delta \pi^+ p \to K^0_S + X$
$\langle K^0_S \rangle = 0.21 \pm 0.02$
$\langle K^0_S \rangle_n = (0.002 \pm 0.004) n_{ch} + (0.18 \pm 0.05)$
$\chi^2 = 23/10$ df
○ $K^+ p \to K^0_S + X$
$\langle K^0_S \rangle = 0.21 \pm 0.03$
$\langle K^0_S \rangle_n = (-0.005 \pm 0.008) n_{ch} + (0.27 \pm 0.08)$
$\chi^2 = 6.8/6$ df
$\langle K^0_S \rangle_n$
n_{ch}
0
0.2
0.4
0.6
4
8
12
16
20

Fig. 1(a)

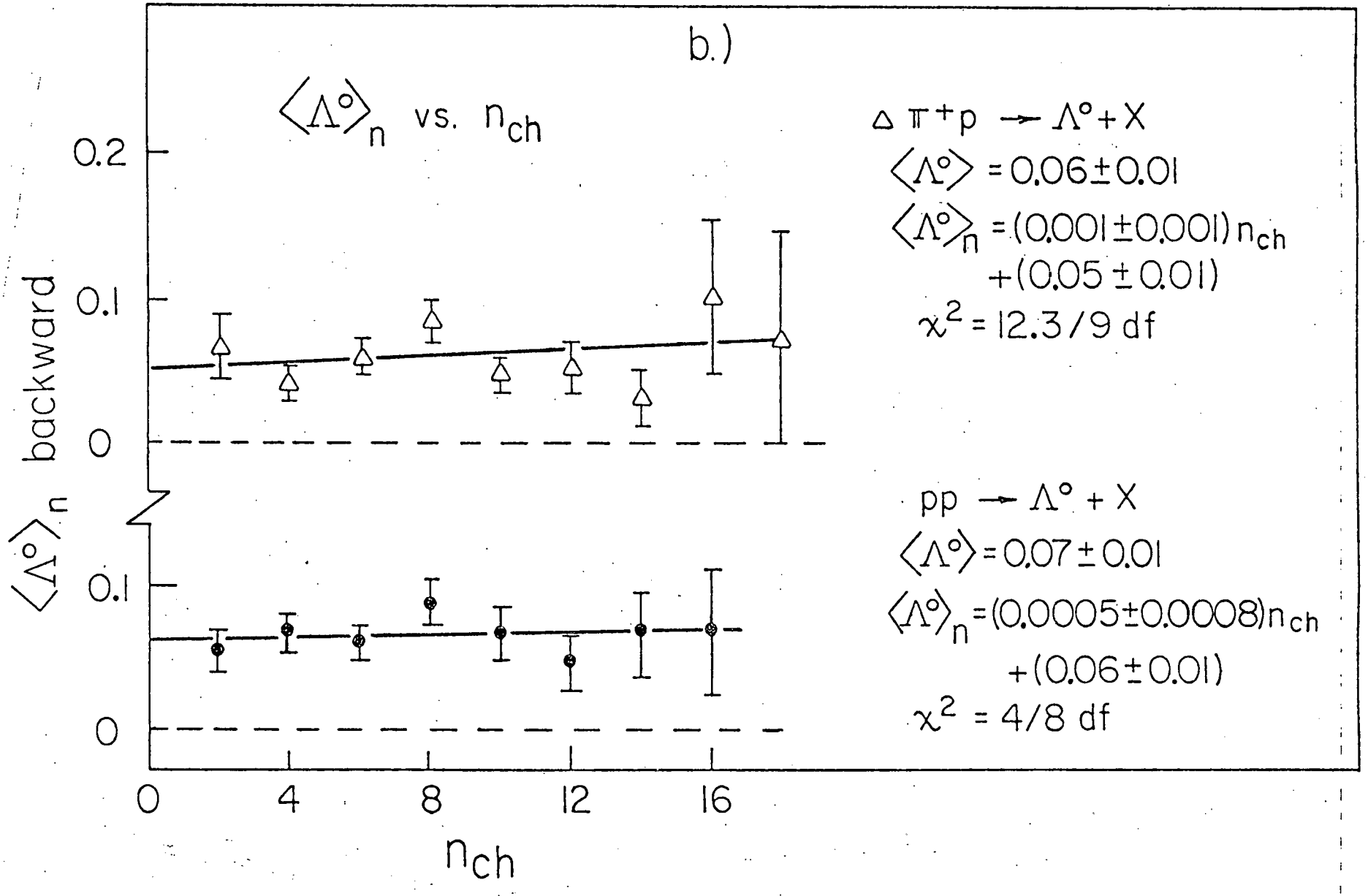
b.)
$\langle \Lambda^\circ \rangle_n$ vs. n_{ch}
$\Delta\ \pi^+ p \rightarrow \Lambda^\circ + X$
$\langle \Lambda^\circ \rangle = 0.06 \pm 0.01$
$\langle \Lambda^\circ \rangle_n = (0.001 \pm 0.001)\, n_{ch} + (0.05 \pm 0.01)$
$\chi^2 = 12.3/9$ df
$pp \rightarrow \Lambda^\circ + X$
$\langle \Lambda^\circ \rangle = 0.07 \pm 0.01$
$\langle \Lambda^\circ \rangle_n = (0.0005 \pm 0.0008)\, n_{ch} + (0.06 \pm 0.01)$
$\chi^2 = 4/8$ df
$\langle \Lambda^\circ \rangle_n$ backward
0.2
0.1
0
0.1
0
0
4
8
12
16
n_{ch}

Fig. 1(b)

K_s produced per inelastic collison is 0.15 ± 0.01 for the proton collisions, 0.21 ± 0.02 for the π^+ beam, and 0.21 ± 0.03 for the K^+ beam. For reaction (2), the K_s with rapidity >1.5 have been excluded from this calculation in order to concentrate on central region production. This difference in $\langle K_s \rangle$ seems to indicate that the two mesons produce more K_s in the central region than do proton beams. This result has previously been observed in charged particle production by different beam types, although the effect was not as pronounced as it appears to be in K_s production. One explanation for the higher multiplicity of particles in meson collisions than that from proton beams may be derived from constituent model considerations. If multiparticle production is a result of constituent interactions, then the available energy of the consitutents involved in a meson-proton collision is presumed to be higher than that for proton-proton collisions. Empirically it has been observed that average multiplicity increases with available energy. Therefore, one expects higher multiplicities from the more catastrophic meson-proton interactions. Another possible reason for the discrepancy is the contribution from the quark-antiquark annihilation process which is allowed in the meson interactions and absent in proton collisions.

Figure 2(a), (b), (c) shows the topological cross sections plotted according to the semi-inclusive Koba-Nielsen-Olesen (KNO) scaling equation[10]

$$\frac{\langle n_c \rangle}{\langle n_v \rangle} \frac{\sigma_n(V^o)}{\sigma_{inel.}} = \phi \left(\frac{n_c}{\langle n_c \rangle}\right) ,$$

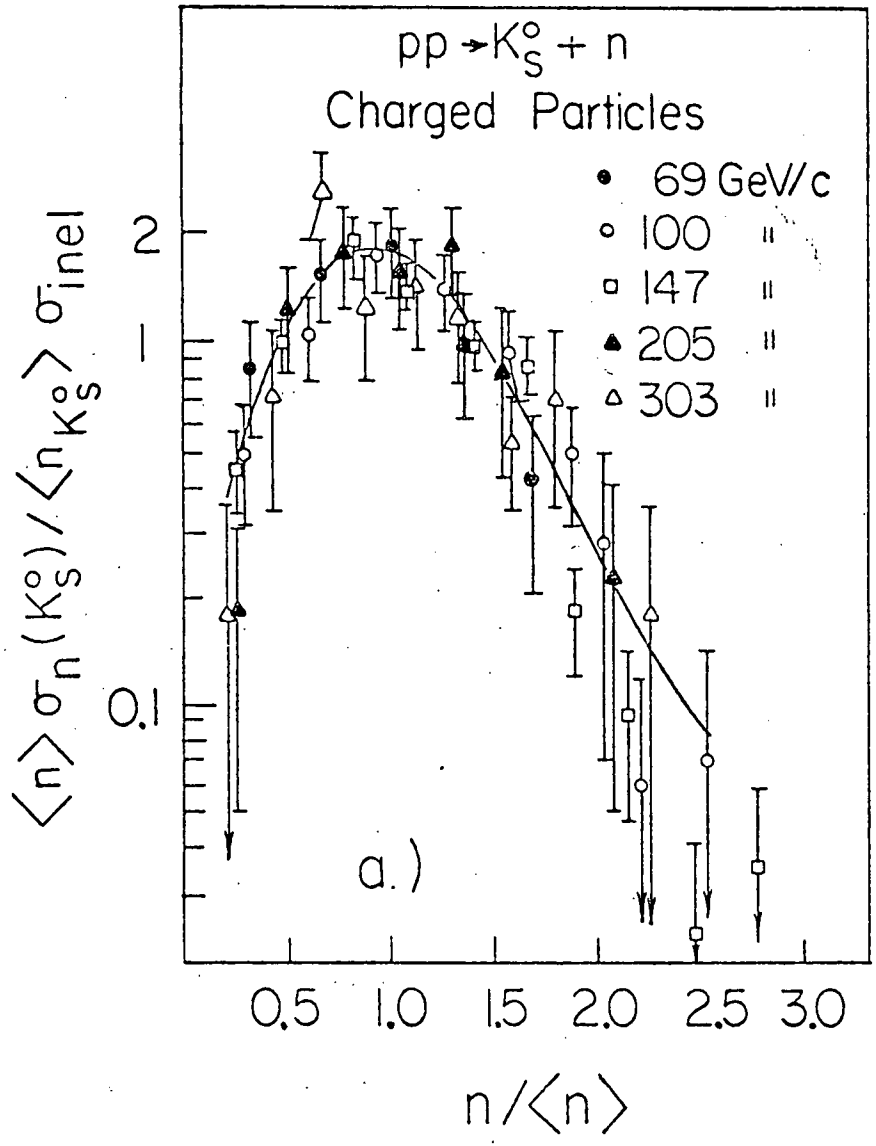
pp → K°S + n
Charged Particles
69 GeV/c
100
147
205
303
a.)
⟨n⟩ σn (K°S) / ⟨nK°S⟩ σinel
n/⟨n⟩
0.5
1.0
1.5
2.0
2.5
3.0
2
1
0.1

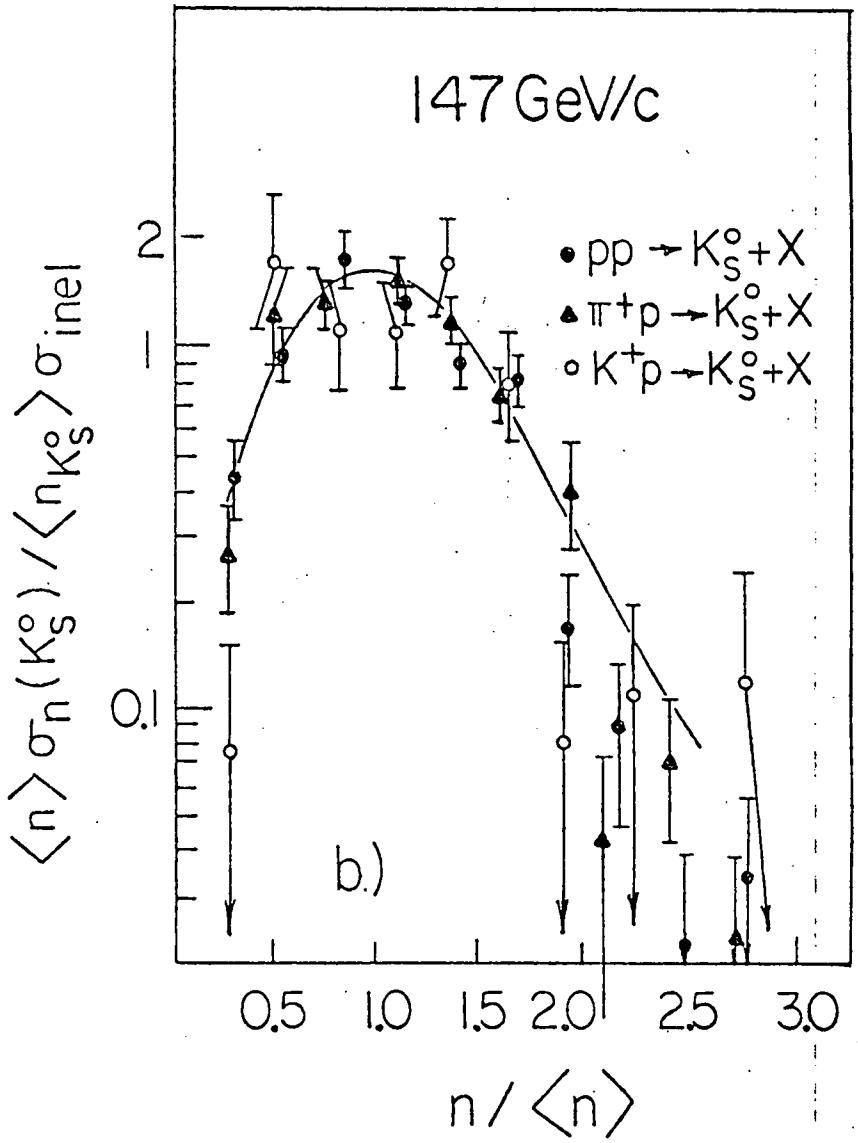
147 GeV/c
pp → K°S+X
π+p → K°S+X
K+p → K°S+X
b.)
⟨n⟩ σn (K°S) / ⟨nK°S⟩ σinel
n/⟨n⟩
0.5
1.0
1.5
2.0
2.5
3.0
2
1
0.1

Fig. 2 (a, b)

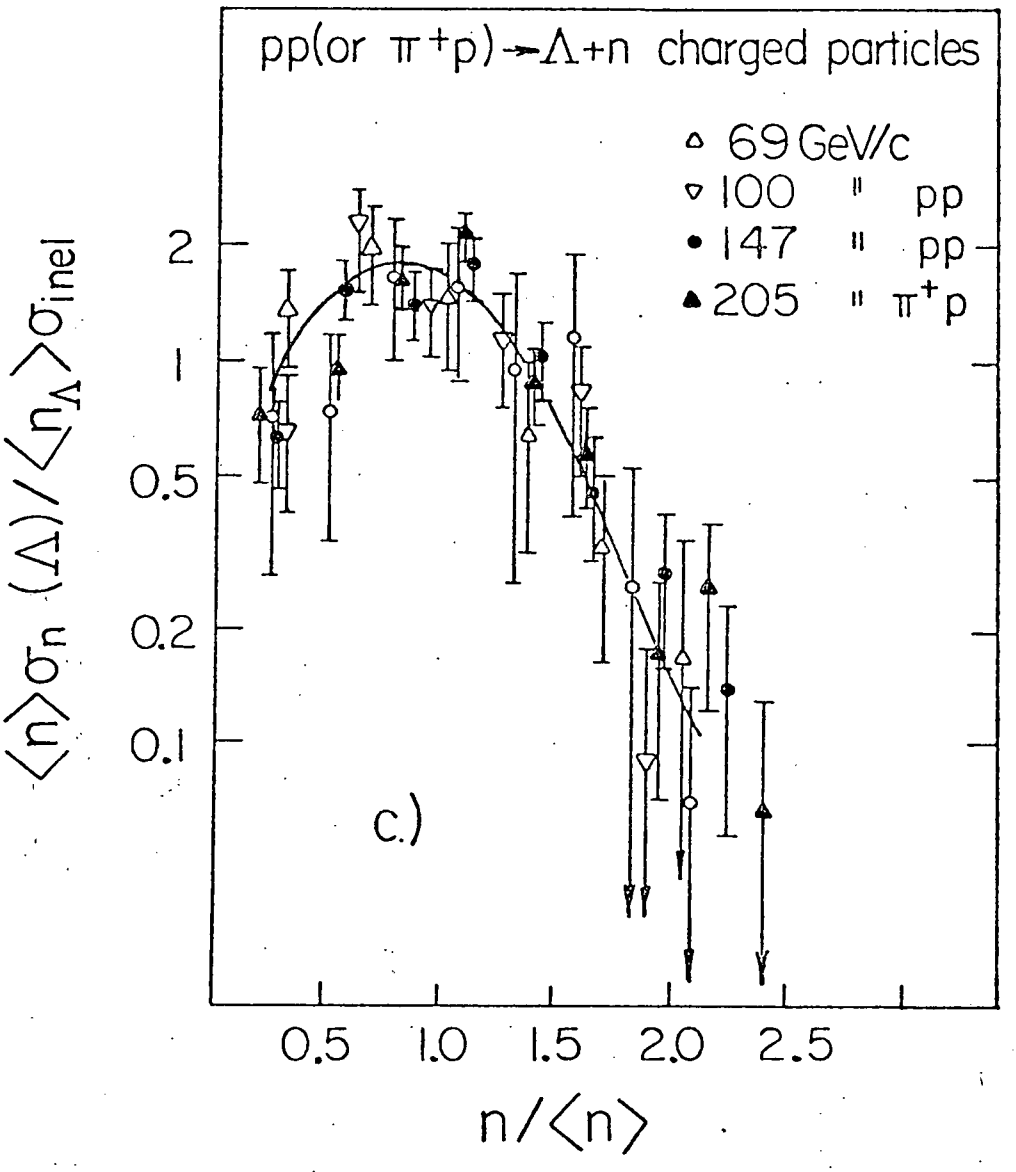
pp(or π⁺p)→Λ+n charged particles
△ 69 GeV/c
▽ 100 " pp
• 147 " pp
▲ 205 " π⁺p
c.)
⟨n⟩σn (Λ)/⟨nΛ⟩σinel
2
1
0.5
0.2
0.1
0.5
1.0
1.5
2.0
2.5
n/⟨n⟩

Fig. 2(c)

where $\langle n_c \rangle$ and $\langle n_v \rangle$ are the average numbers of charged particles and V^o particles respectively, $\sigma_n(V^o)$ is the inclusive topological cross section for production of the V^o with n charged prongs, $\sigma_{inel.}$ is the total inelastic cross section, and ϕ is, according to the scaling hypothesis, an energy-independent function.

Cohen has plotted results from pp collisions in the energy range 69 - 303 GeV/c for K_s production and 69 - 205 GeV/c for Λ production.[11] These data indicate that there is little or no energy dependence of the function ϕ, as predicted by the KNO scaling hypothesis. In Figure 2(b), we show the results from this experiment only. Our data from pp collisions agree with that reported by Cohen, and this experiment shows no detectable difference in the data from different beam types at the same energy. Furthermore, there appears to be no significant difference in the data between K_s and Λ production. There is no reason to expect that the function ϕ would be the same for these two particles, since they are produced by quite different mechanisms. The K_s production occurs predominantly in the central region of rapidity space, due presumably to the combination of two "sea" quarks, while Λ production is the result of target fragmentation and is generally supposed to be the combination of two of the valence quarks of the proton with a sea quark.

In Figure 3(a) the rapidity distribution in the backward hemisphere of K_s produced in pp collisions at 147 GeV/c (this experiment) is compared with the distribution of K_s produced in pp collisions at 300 GeV/c.[6] These plots clearly indicate that K_s production occurs in the central

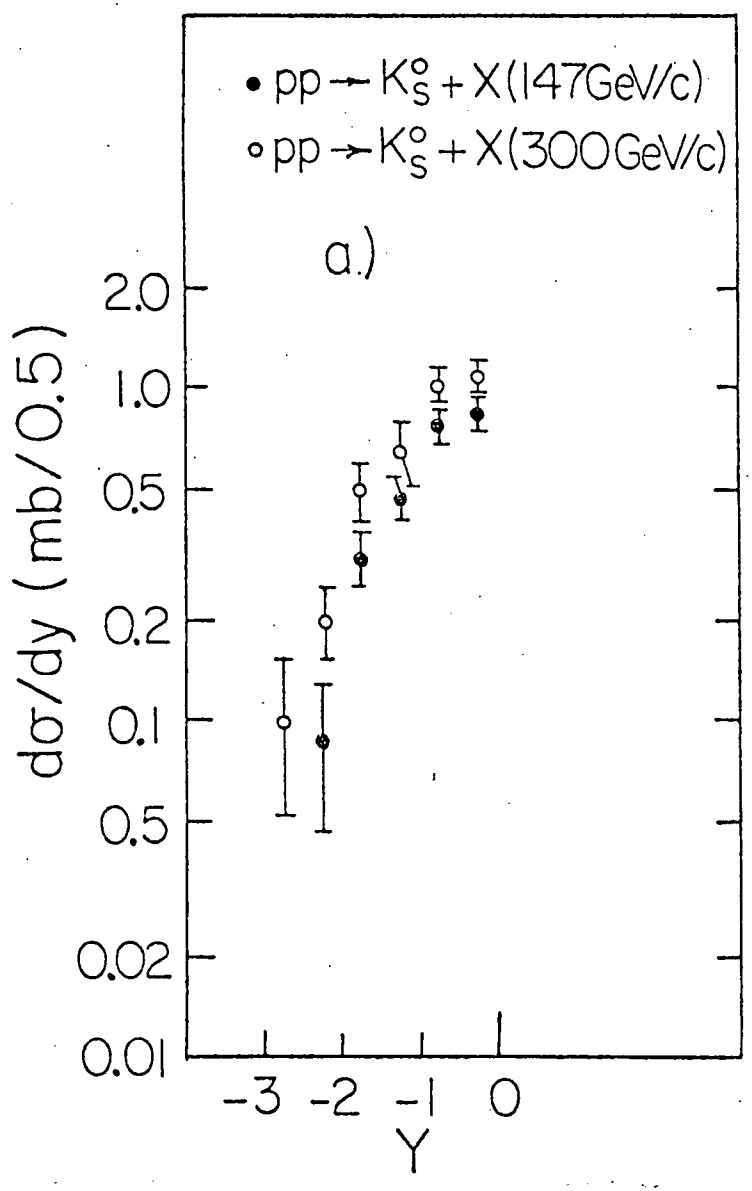
• pp → K°s + X(147GeV/c)
∘ pp → K°s + X(300GeV/c)
a.)
dσ/dy (mb/0.5)
2.0
1.0
0.5
0.2
0.1
0.5
0.02
0.01
-3 -2 -1 0
Y

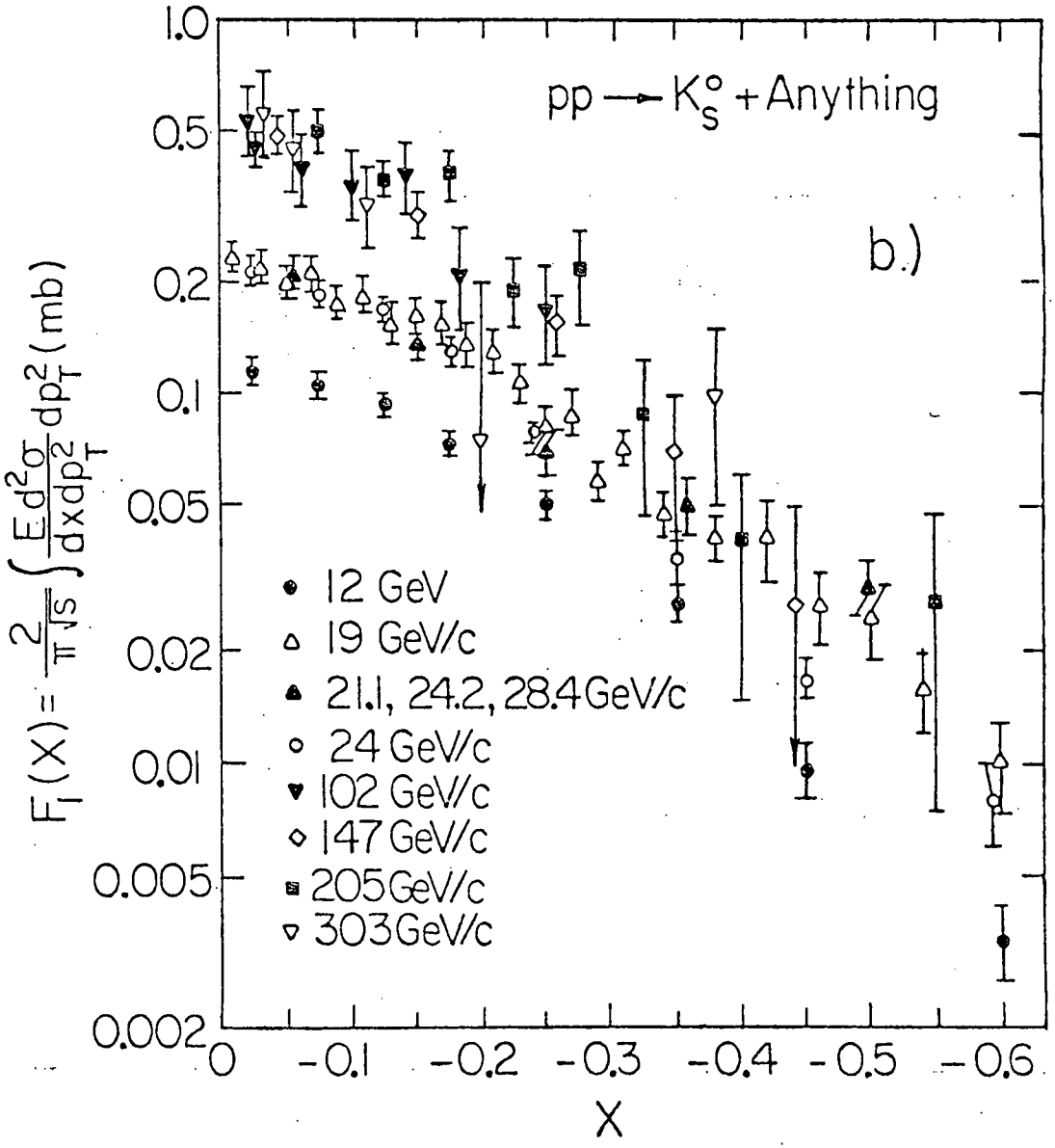
pp → K°s + Anything
b.)
$F_1(X) = \frac{2}{\pi\sqrt{s}} \int \frac{E d^2\sigma}{dx dp_T^2} dp_T^2$ (mb)
1.0
0.5
0.2
0.1
0.05
0.02
0.01
0.005
0.002
0 -0.1 -0.2 -0.3 -0.4 -0.5 -0.6
X
12 GeV
19 GeV/c
21.1, 24.2, 28.4GeV/c
24 GeV/c
102 GeV/c
147 GeV/c
205GeV/c
303GeV/c

Fig. 3

region of rapidity space. The shapes of these two curves are the same, and there is no indication of a central region plateau in either one. The formation of the central region plateau with increasing energy should be characterized by the broadening of the central region. This is not the case here, so it may be concluded that, at presently accessible energies, there is no indication of the central region plateau expected as a consequence of the multi-peripheral model.

The backward-hemisphere Feynman x distributions of K_s production from pp collisions at different energies[12] are presented in Figure 3(b). From this collection of data it may be conjectured that scaling in the Feynman x variable has begun by 150 GeV/c in pp collisions, possibly by 100 GeV/c. The scaling is approached from below; that is, as the energy of the beam increases, the height of the distribution also increases, until there is no observable change in the distribution from about 100 GeV/c to 300 GeV/c.

The rapidity distribution for K_s production from π^+ beams at 147 GeV/c is plotted in Figure 4(a), along with the distribution from π^- beams at the same energy, obtained in E-154. The distributions are identical, within the experimental uncertainties, indicating that K_s production may proceed via the same mechanism in π^+p and π^-p collisions.

Figure 4(b) shows the Feynman x distribution for inclusive K_s production at 147 GeV/c in π^+p collisions. This plot makes it obvious that K_s production in π^+p collisions is not symmetric about $x = 0$, but has a larger cross section for $x > 0$ than for $x < 0$. This forward shift has been observed before, as indicated by the data on the same graph from an 18.5 GeV/c π^-p experiment.[13]

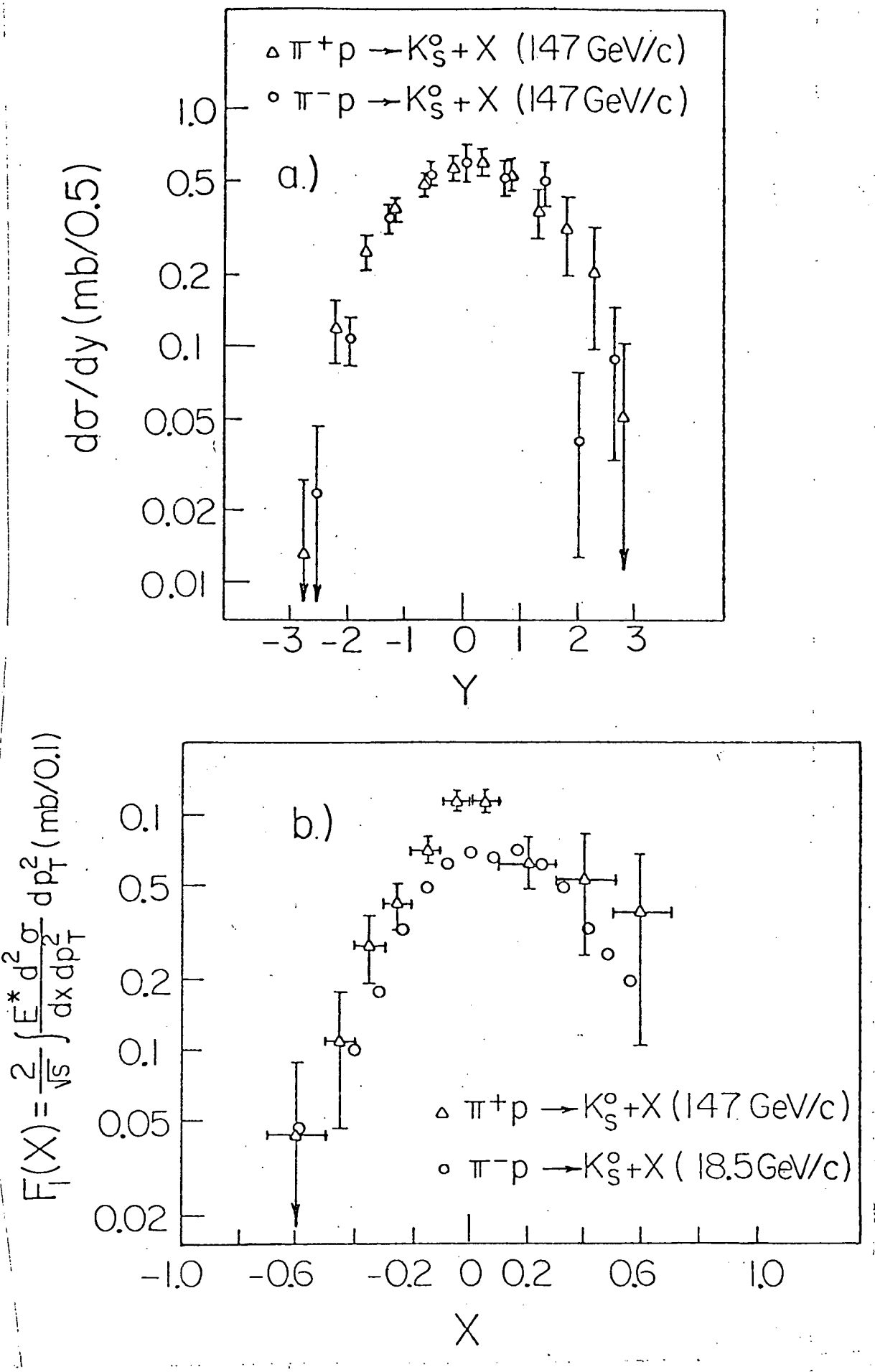
△ π⁺p → K°S + X (147 GeV/c)
○ π⁻p → K°S + X (147 GeV/c)
a.)
dσ/dy (mb/0.5)
1.0
0.5
0.2
0.1
0.05
0.02
0.01
-3 -2 -1 0 1 2 3
Y
b.)
$F_1(X) = \frac{2}{\sqrt{s}} \int \frac{E^* d^2\sigma}{dx\, dp_T^2} dp_T^2$ (mb/0.1)
0.1
0.5
0.2
0.1
0.05
0.02
△ π⁺p → K°S + X (147 GeV/c)
○ π⁻p → K°S + X (18.5 GeV/c)
-1.0 -0.6 -0.2 0 0.2 0.6 1.0
X

Fig. 4

In Figure 5 the rapidity and Feynman x distributions for K_s production from reaction (2) are shown. Although the experimental uncertainties for these distributions are larger than those for reaction (1) and (3) due to lower statistics, several observations may be made about these spectra. First, one expects a large contribution to the inclusive K_s cross section from diffractive beam dissociation events where the initial strangeness of the beam is carried through as a fast K_s. From this figure, it appears as if the beginning of the forward peak is visible; however, there are several systematic reasons for the fact that we have been unable to observe many fast K_s in this data sample. The number of K^+ beam events is small, and the very fast K_s produced will almost always decay outside the bubble chamber. A crude calculation shows that, in the data sample used, one expects to see only one or two of these fast K_s. Just one K_s in the chamber with a momentum of 120 GeV/c would add approximately 0.7 mb to the K_s cross section, increasing it by over ten per cent.

One other observation may be made about the K_s distributions. For the rapidity region $y < 1.5$ and the Feynman x region $x \lesssim 0.2$, the K_s spectra from the K^+ beam match those from the π^+ beam. The heights of the plots at $x = 0$ and $y = 0$ are the same, and they fall off from zero at the same rate. This implies that the production of central region K_s is the same for π^+p and π^-p collisions as it is for K^+p collisions.

The invariant Feynman x distributions for Λ's produced in reactions (4)-(6) are shown in Fig. 6. It is evident that there is a peak in inclusive production at $x \sim -0.5$ or -0.6 for all three types of beams.

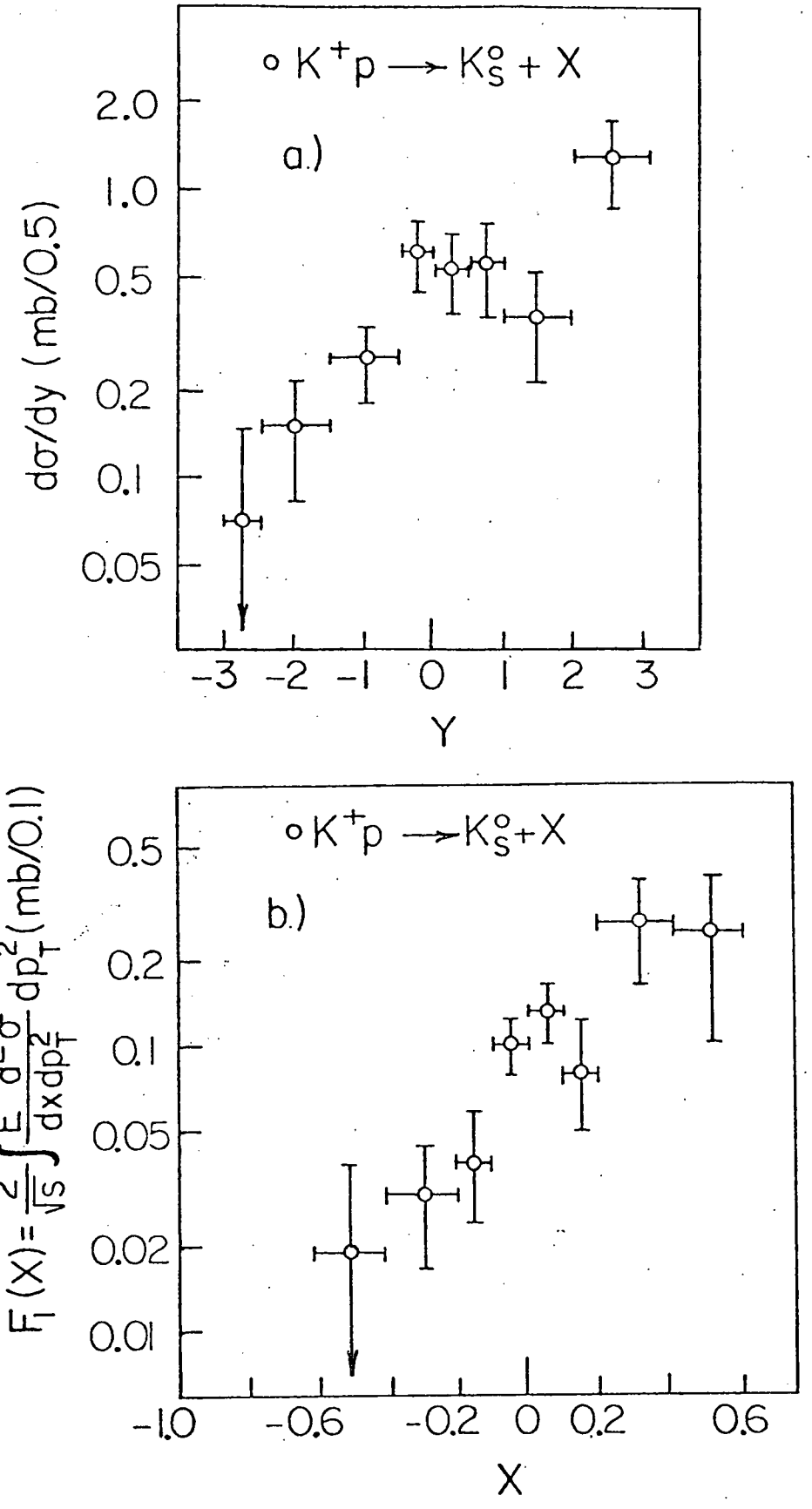
o K+p → Ks° + X
a.)
dσ/dy (mb/0.5)
2.0
1.0
0.5
0.2
0.1
0.05
-3 -2 -1 0 1 2 3
Y
o K+p → Ks° + X
b.)
F1(X) = 2/√s ∫ E* d²σ/dx dp_T² dp_T² (mb/0.1)
0.5
0.2
0.1
0.05
0.02
0.01
-1.0 -0.6 -0.2 0 0.2 0.6
X

Fig. 5

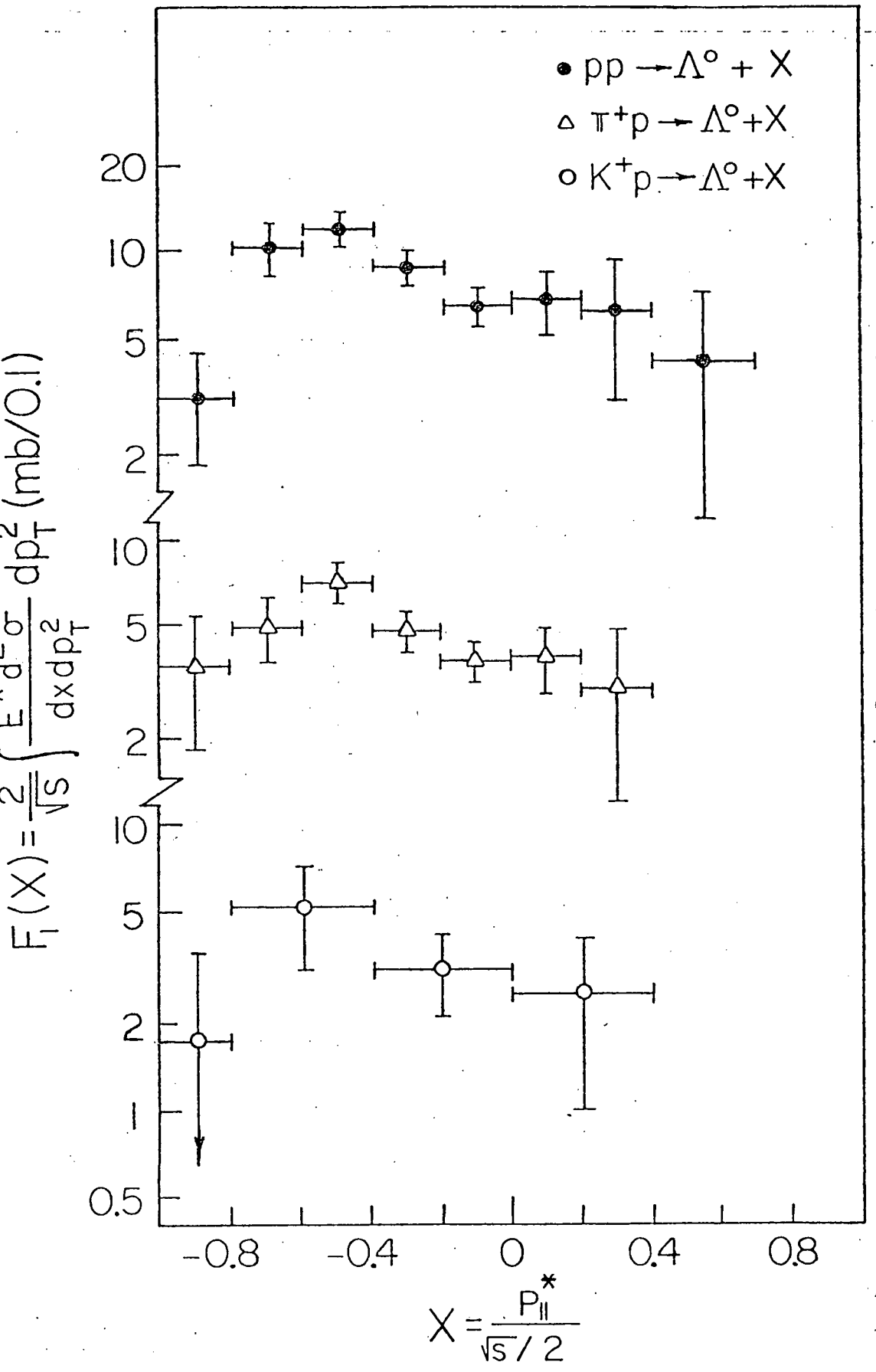
pp → Λ° + X
π⁺p → Λ°+X
K⁺p → Λ°+X
20
10
5
2
10
5
2
10
5
2
1
0.5
-0.8
-0.4
0
0.4
0.8
$F_1(X) = \frac{2}{\sqrt{s}} \int \frac{E^* d^2\sigma}{dx\, dp_T^2} dp_T^2$ (mb/0.1)
$X = \frac{P_{\parallel}^*}{\sqrt{s}/2}$

Fig. 6

Furthermore, there is some central region production of Λ and the height of the Feynman x distribution at x = 0 is approximately one-half of that of the backward peak in all three beam types. In fact, the three plots are similar to one another, and, within experimental errors, the shapes appear to be consistent with one another, apart from the overall normalization.

The production of Λ's from the proton beam should be symmetric about x = 0, but we observe that this is true only out to about x = 0.4. This is another result of the systematic bias against detection of fast-forward neutral particles. The backward hemisphere distribution of Feynman x for pp collisions at different energies[12] is shown in Figure 7. From this figure, it is evident that Feynman scaling in inclusive Λ production by protons has been achieved by a lab momentum of at most 100 GeV/c.

Rapidity distributions for reactions (4) and (5) are shown in Figure 8, along with that from E-154. The two pion experiments are consistent with one another, within experimental errors. As with the centrally-produced K_s, the target-fragmentation and central Λ's produced by meson beams are quite similar.

The $\bar{\Lambda}$ rapidity distributions for this experiment are shown in Figure 9(a), and the Feynman x distributions are shown in Figure 9(b). From these plots, it is evident that $\bar{\Lambda}$ production takes place in the central region. The heights of the plots at y = 0 and at x = 0 are consistent with being the same for the two meson beams, as well as being consistent with that from the π^- experiment at the same energy. The same

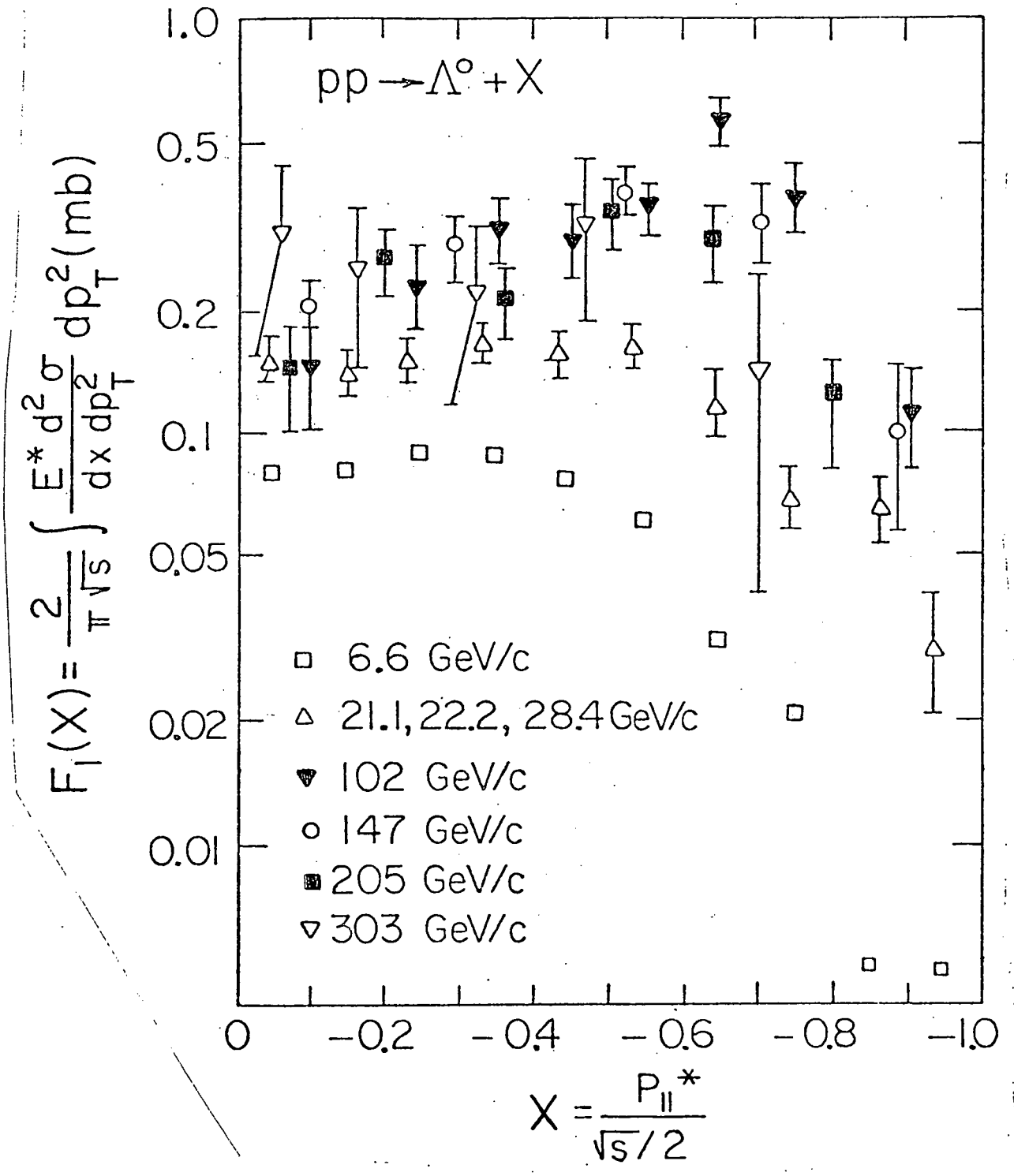
pp → Λ° + X
1.0
0.5
0.2
0.1
0.05
0.02
0.01
0
−0.2
−0.4
−0.6
−0.8
−1.0
6.6 GeV/c
21.1, 22.2, 28.4 GeV/c
102 GeV/c
147 GeV/c
205 GeV/c
303 GeV/c
$F_1(X) = \frac{2}{\pi\sqrt{s}} \int \frac{E^* d^2\sigma}{dx\, dp_T^2} dp_T^2 (mb)$
$X = \frac{P_{||}^*}{\sqrt{s}/2}$

Fig. 7

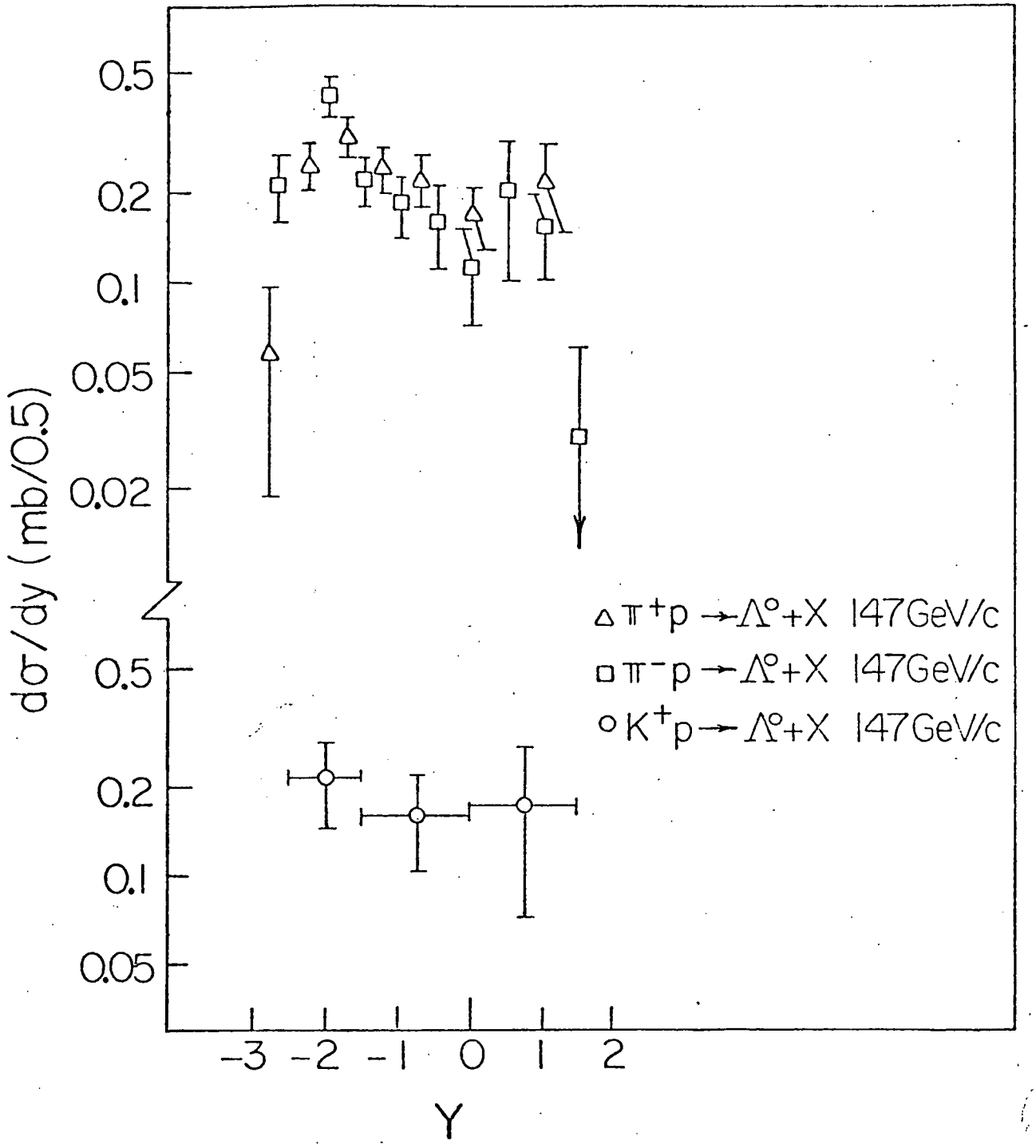
0.5
0.2
0.1
0.05
0.02
0.5
0.2
0.1
0.05
dσ/dy (mb/0.5)
△ π+p → Λ°+X 147GeV/c
□ π-p → Λ°+X 147GeV/c
○ K+p → Λ°+X 147GeV/c
-3
-2
-1
0
1
2
Y

Fig. 8

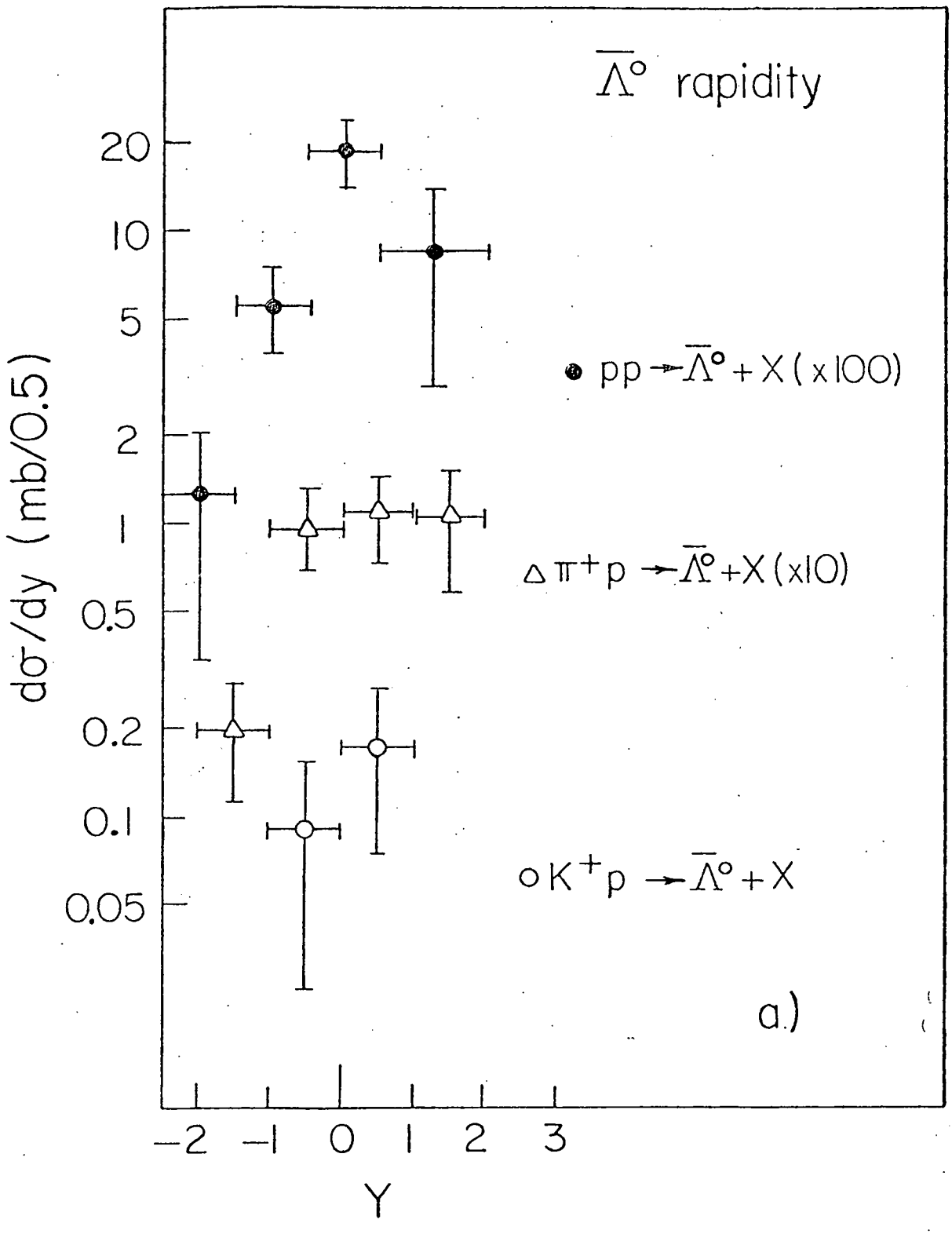
$\bar{\Lambda}^0$ rapidity
20
10
5
2
1
0.5
0.2
0.1
0.05
$d\sigma/dy$ (mb/0.5)
$pp \rightarrow \bar{\Lambda}^0 + X$ (x100)
$\Delta \pi^+ p \rightarrow \bar{\Lambda}^0 + X$ (x10)
$K^+ p \rightarrow \bar{\Lambda}^0 + X$
a.)
−2
−1
0
1
2
3
Y

Fig. 9(a)

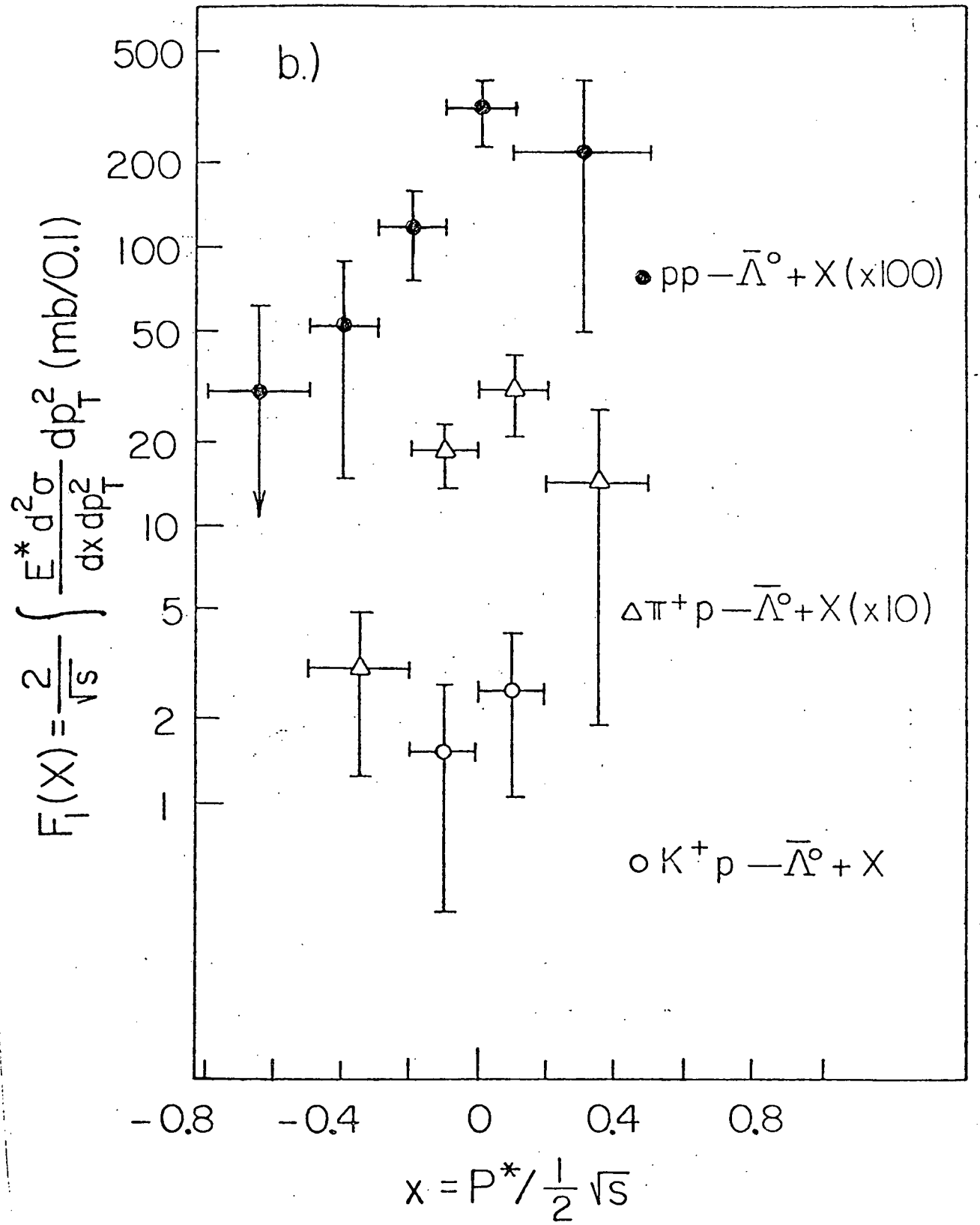
b.)
500
200
100
50
20
10
5
2
1
$F_1(X) = \frac{2}{\sqrt{s}} \int \frac{E^* d^2\sigma}{dx\, dp_T^2} dp_T^2$ (mb/0.1)
● $pp \to \bar{\Lambda}^0 + X$ (x100)
△ $\pi^+ p \to \bar{\Lambda}^0 + X$ (x10)
○ $K^+ p \to \bar{\Lambda}^0 + X$
-0.8
-0.4
0
0.4
0.8
$x = P^* / \frac{1}{2}\sqrt{s}$

Fig. 9(b)

result was observed in K_s production, which also occurs in the central region. The cross sections for both K_s and $\bar{\Lambda}$ production are rising at these energies, and there is no evidence in either case for a central region plateau.

It is interesting to note that the values of $d\sigma/dy$ at $y = 0$ for Λ° are consistently higher for each beam than the corresponding values for $\bar{\Lambda}$. This indicates that central region Λ production is not solely the result of $\Lambda\bar{\Lambda}$ production. It may be that some of the central region Λ's are the result of a "tail" of target fragmentation production.

REFERENCES

1. M. Alston-Garnjost et al., Phys. Rev. Lett. 35, 142 (1975).
2. J. Chapman et al., Phys. Lett. 47B, 465 (1973).
3. G. Charlton et al., Phys. Rev. Lett. 30, 574 (1973).
4. K. Jaeger et al., Phys. Rev. D11, 2405 (1975).
5. F. Dao et al., Phys. Rev. Lett. 30, 1151 (1973).
6. A. Sheng et al., Phys. Rev. D11, 1733 (1975).
7. H. Kichini et al., Phys. Lett. 72B, 411 (1978).
8. J. Whitmore, Physics Reports 27C, 187 (1976). (Review Article).
9. R. D. Field and R. P. Feynman, Nucl. Phys. B136, 1 (1978).
10. F. T. Dao and J. Whitmore, Phys. Lett. 46B, 252 (1973).
11. D. Cohen, Phys. Lett. 47B, 457 (1973).
12. Data other than this experiment are taken from J. Whitmore, Physics Reports 10C, 273 (1974).
13. P. H. Stuntebeck et al., Phys. Rev. D9, 608 (1974).

(iii) Single Charged-Particle Distributions in x and y, from π^+p, K^+p, and pp Interactions at 147 GeV/c.

This work was the subject of a contributed paper presented at the 1979 Washington meeting of the APS by Mildred Widgoff.

The invariant distributions in rapidity y, $\rho = (1/\sigma_T)d\sigma/dy$, determined for the three different particles in the beam, provide an excellent test of the degree of dependence or independence of the secondary spectra on the quantum numbers of the incident particle. In particular, the results allow one to check the factorization of the cross section as given by Mueller-Regge theory. Figure 1 shows Mueller diagrams for particle production in the target fragmentation region and in the central region of rapidity y, for reactions of the type $ab \to cX$.

Consider first production in the fragmentation region, represented in Fig. 1(a). According to Mueller-Regge: If the pomeron dominates the exchange between particles a and c, and if the cross section is factorizable, then the cross section for production of c in the fragmentation region of the target a can be written[1-3] in the form of a product of two terms:

$$d^2\sigma/dydp_T^2 = \beta_{ac}(y,p_T^2)\ \beta_b \quad . \tag{1}$$

This is analogous to the factorization of the total cross section for interactions a+b, which can be written in the form

$$\sigma_T = \beta_a\ \beta_b \quad . \tag{2}$$

MUELLER DIAGRAMS

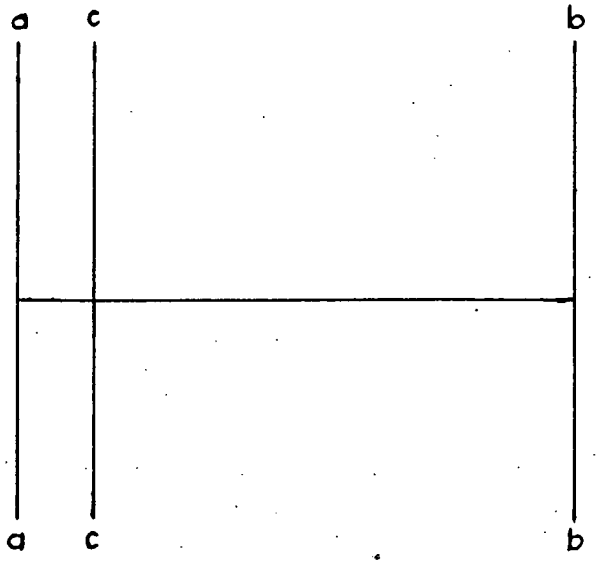

(a) Production in Fragmentation Region

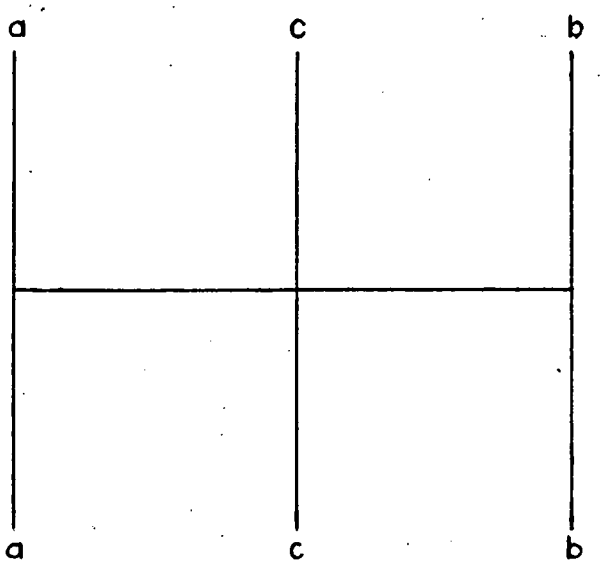

(b) Production in Central Region

Fig. 1

Dividing Equation (1) by Equation (2), we find

$$\frac{1}{\sigma_T}\frac{d^2\sigma}{dydp_T^2} = \beta_{ac}(y,p_T^2)/\beta_a \quad , \tag{3}$$

independent of the beam particle b. Inclusion of Reggeon exchanges adds a term with an $s^{-1/2}$ dependence.

For production in the central region, if the pomeron dominates both ac and bc exchanges, we can write

$$d^2\sigma/dydp_T^2 = \beta_c(p_T^2)\ \beta_a\ \beta_b \quad . \tag{4}$$

Dividing Equation (4) by Equation (2), we then obtain

$$\frac{1}{\sigma_T}\frac{d^2\sigma}{dydp_T^2} = \beta_c(p_T^2) \quad , \tag{5}$$

independent of both target and projectile. Inclusion of Regge trajectories adds terms with $s^{-1/4}$ and $s^{-1/2}$ dependences. The conditions of pomeron exchange dominance and factorizability are expected to be satisfied at lower energies for $ab\bar{c}$ exotic, than for $ab\bar{c}$ not exotic.

Figure 2 shows our experimental y spectra separately for π^+ and π^- produced in π^+p, K^+p, and pp interactions. Actually plotted are the structure functions $\rho(y) = (1/\sigma_T)d\sigma/dy$, summed over all p_T.

Although the π^+ spectra look somewhat asymmetric, the forward/backward ratios for each of the distributions is very close to 1, and the median point for each is very close to 0. The resolution of the histograms is not sufficient to show any small shift in the center point to $y' = 0$ in a quark-quark frame, but they are not inconsistent with a shift of one bin width, $<\sim 0.2$ units in y.

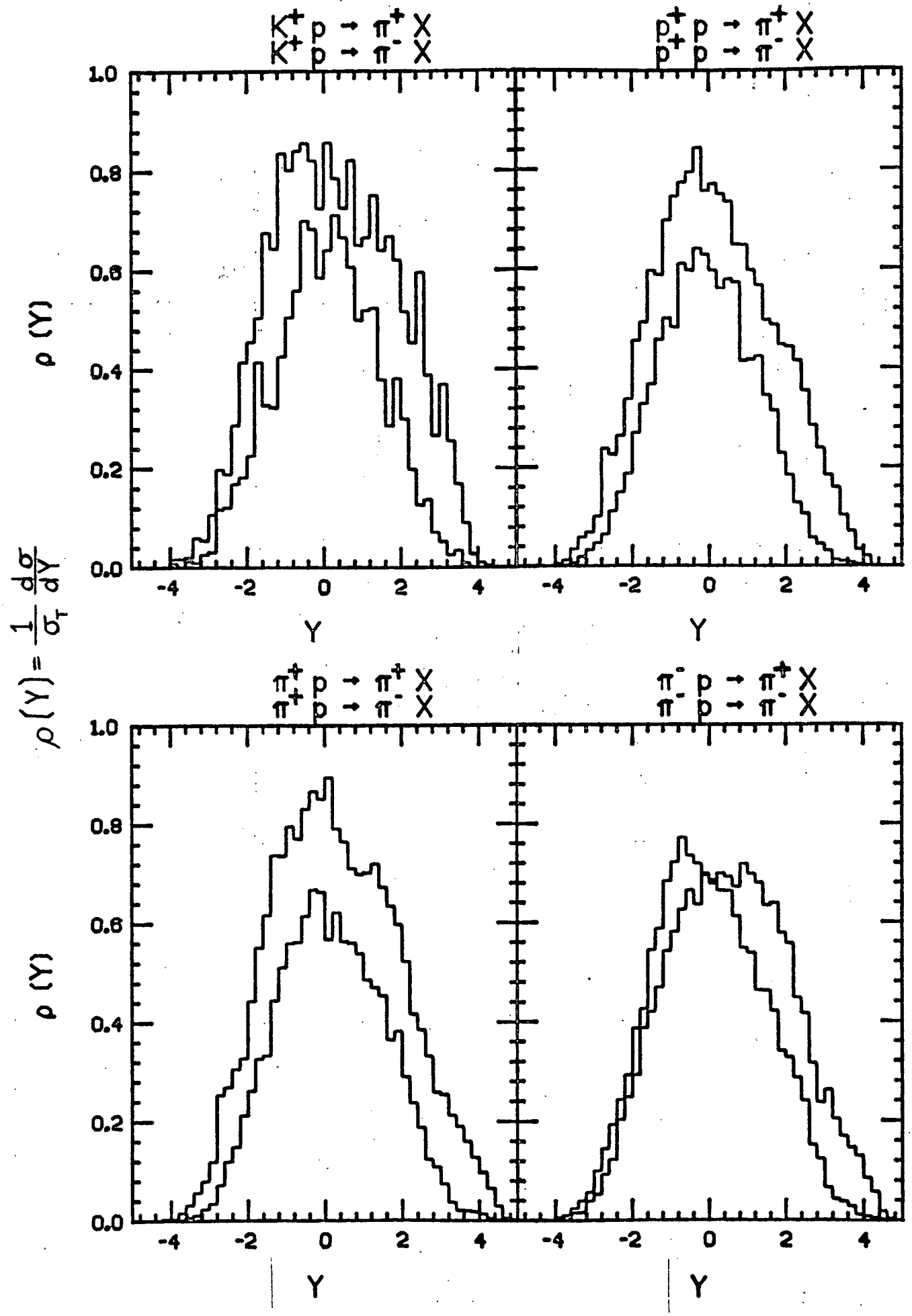
$K^+ p \to \pi^+ X$
$K^+ p \to \pi^- X$
$p^+ p \to \pi^+ X$
$p^+ p \to \pi^- X$
$\pi^+ p \to \pi^+ X$
$\pi^+ p \to \pi^- X$
$\pi^- p \to \pi^+ X$
$\pi^- p \to \pi^- X$
$\rho(Y) = \frac{1}{\sigma_T} \frac{d\sigma}{dY}$
$\rho(Y)$
Y
1.0
0.8
0.6
0.4
0.2
0.0
-4
-2
0
2
4

Fig. 2

There is a problem in the forward hemisphere in the case of pp interactions. We have at present no way to identify fast protons in order to remove them from the π^+ spectrum. Slow protons on the other hand, with momentum up to 1.4 GeV/c, are easily identified and removed. To get $pp \to \pi^+$, we have in this analysis called the fastest forward-going particle a proton and removed it from the $pp \to \pi^+$ plots, provided it is really a leading particle and has $x \gtrsim 0.7$. The result of this is a distortion of the $y > 0$ portion of the $pp \to \pi^+$ spectrum, with some protons remaining but treated as pions, and some pions wrongly removed. This problem does not affect the analysis of the $y < 0$ region.

In order to compare the results with the Mueller-Regge predictions in the target fragmentation region, $y < 0$, we have checked dependence on the projectile by calculating the following ratios, as functions of y:

$$R_\pi^- (y) = \frac{\rho^{\pi^-}_{\pi^+ p}(y)}{\rho^{\pi^-}_{pp}(y)}, \qquad R_\pi^+ (y) = \frac{\rho^{\pi^+}_{\pi^+ p}(y)}{\rho^{\pi^+}_{pp}(y)},$$

$$R_K^- (y) = \frac{\rho^{\pi^-}_{K^+ p}(y)}{\rho^{\pi^-}_{pp}(y)}, \qquad R_K^+ (y) = \frac{\rho^{\pi^+}_{K^+ p}(y)}{\rho^{\pi^+}_{pp}(y)}.$$

These ratios are plotted in Fig. 3. The reactions $\pi^+ p \to \pi^- X$, $K^+ p \to \pi^- X$, $K^+ p \to \pi^+ X$, and $pp \to \pi^- X$ all have $ab\bar{c}$ exotic, and the values of R in the backward hemisphere for these interactions are indeed about 1.0, showing independence of the projectile particle, while the reaction

$R = \rho_b / \rho_p$

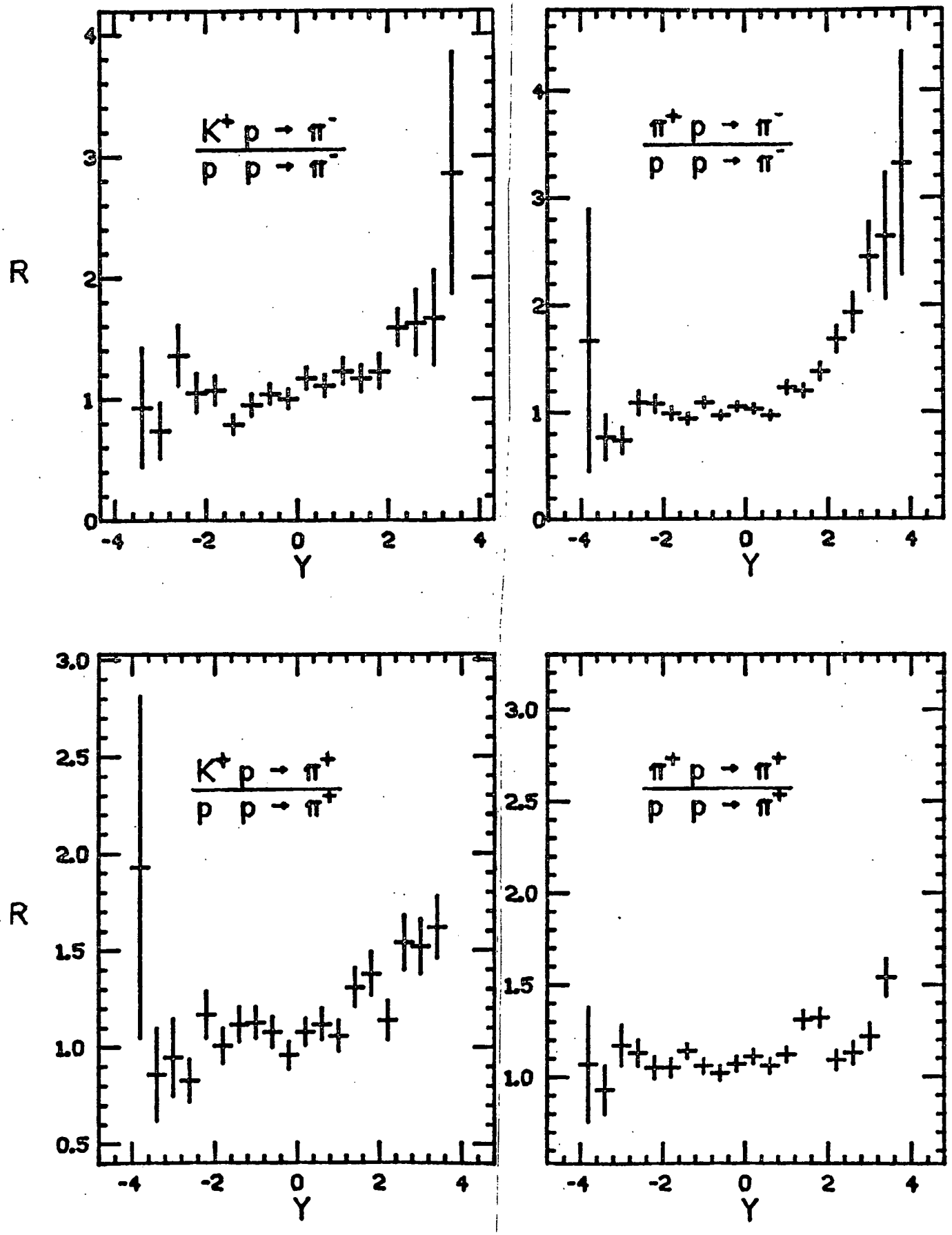

Fig. 3

$\pi^+ p \to \pi^+ X$, where $ab\bar{c}$ is not exotic, is higher than 1.0, slightly but systematically. The average values of R for $y < 0$ are:

$$\left.\begin{aligned} \langle R_\pi^- \rangle &= 0.97 \pm 0.03 \\ \langle R_K^- \rangle &= 0.99 \pm 0.07 \\ \langle R_K^+ \rangle &= 1.01 \pm 0.04 \end{aligned}\right\} \quad ab\bar{c} \text{ exotic}$$

$$\langle R_\pi^+ \rangle = 1.10 \pm 0.03 \qquad ab\bar{c} \text{ not exotic}$$

The average value of R for the non-exotic combination is different from 1.0 by about 3 standard deviations. This ratio should also approach 1.0 as the energy increases. Our data thus confirm the independence of projectile particles for $y < 0$ implied by the Mueller-Regge theory.

In Fig. 4 are shown the invariant cross sections in Feynman x for various reactions $ab \to cX$.

Various quark fragmentation or cascade theories[4-7] predict a $(1-x)^n$ dependence of the invariant cross sections in the region $0.2 \lesssim x < 0.7$ and this has been borne out by a number of experiments. A unique feature of the hybrid system is the accessibility of the whole spectrum in x; we have fitted our distributions to a power law in (1-x), for the two regions of x, both $-0.7 \lesssim x \lesssim -0.2$ and the usual $0.2 \lesssim x < 0.7$. The power law gives a reasonably good fit, as can be seen in Figs. 5 and 6 which show the relevant regions in x enlarged, for $\pi^+ p$ and $K^+ p$ interactions. Similar fits have been made for $pp \to \pi^\pm$ and $\pi^- p \to \pi^\pm$, except for the forward hemisphere in the case of $pp \to \pi^+$, because of the doubtful distinction between forward p and π^+ mentioned earlier.

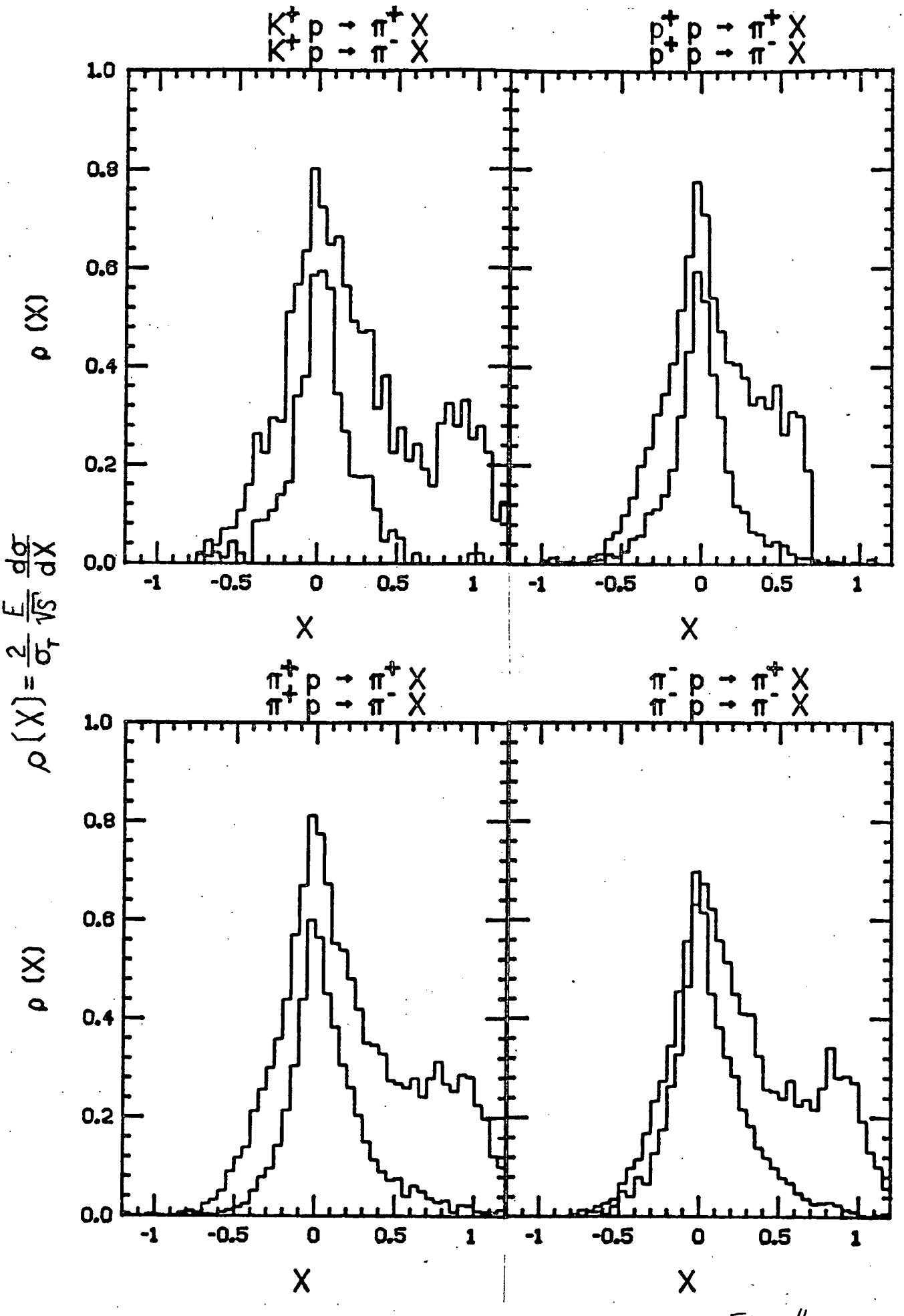
$K^+ p \to \pi^+ X$
$K^+ p \to \pi^- X$
$p^+ p \to \pi^+ X$
$p^+ p \to \pi^- X$
$\pi^+ p \to \pi^+ X$
$\pi^+ p \to \pi^- X$
$\pi^- p \to \pi^+ X$
$\pi^- p \to \pi^- X$
$\rho(X) = \frac{2}{\sigma_T} \frac{E}{\sqrt{s}} \frac{d\sigma}{dX}$
$\rho(X)$
X
1.0
0.8
0.6
0.4
0.2
0.0
-1
-0.5
0
0.5
1

Fig. 4

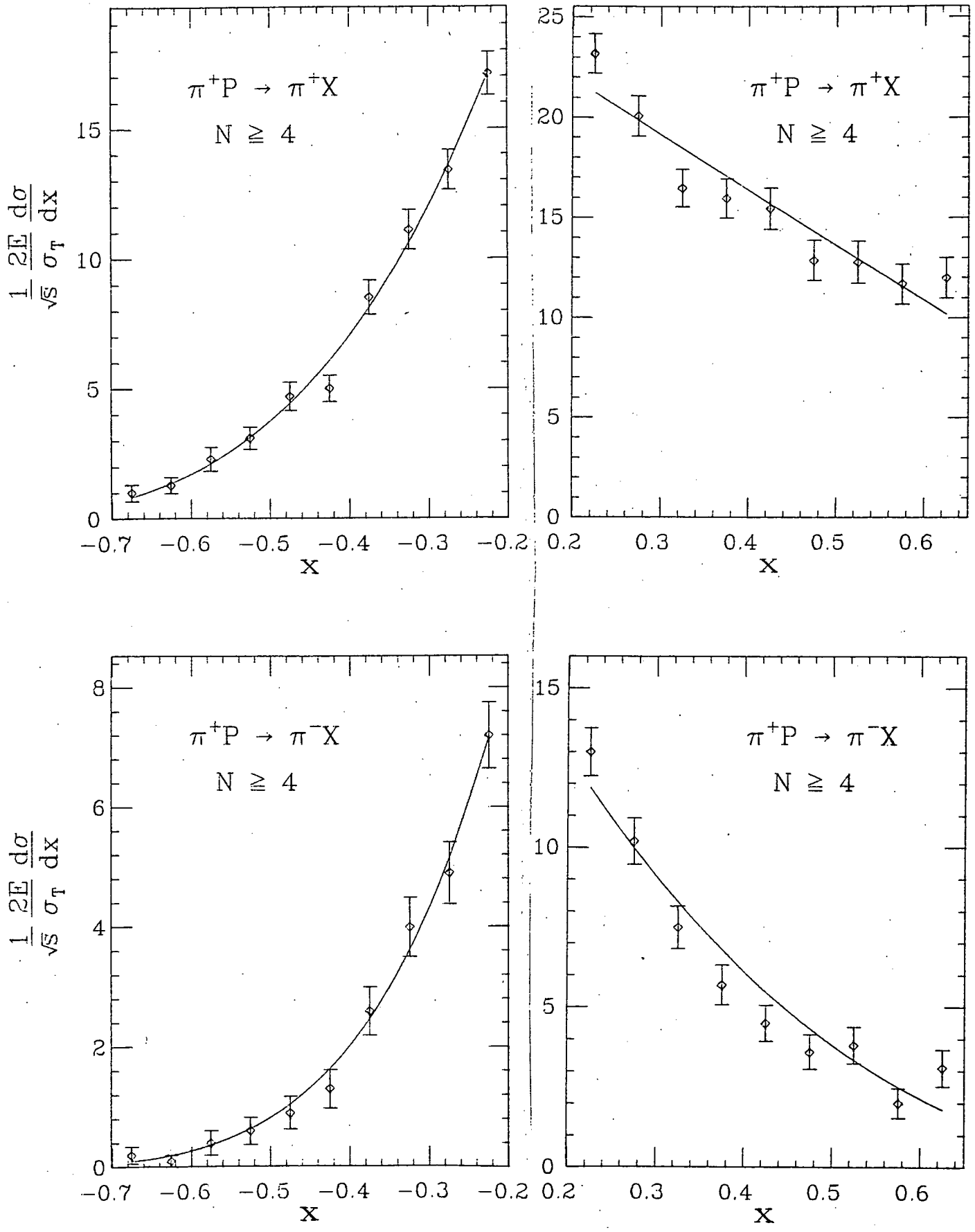
$\pi^+P \rightarrow \pi^+X$
N ≧ 4
$\frac{1}{\sqrt{s}} \frac{2E}{\sigma_T} \frac{d\sigma}{dx}$
x
$\pi^+P \rightarrow \pi^-X$
N ≧ 4
$\frac{1}{\sqrt{s}} \frac{2E}{\sigma_T} \frac{d\sigma}{dx}$
x

Fig. 5

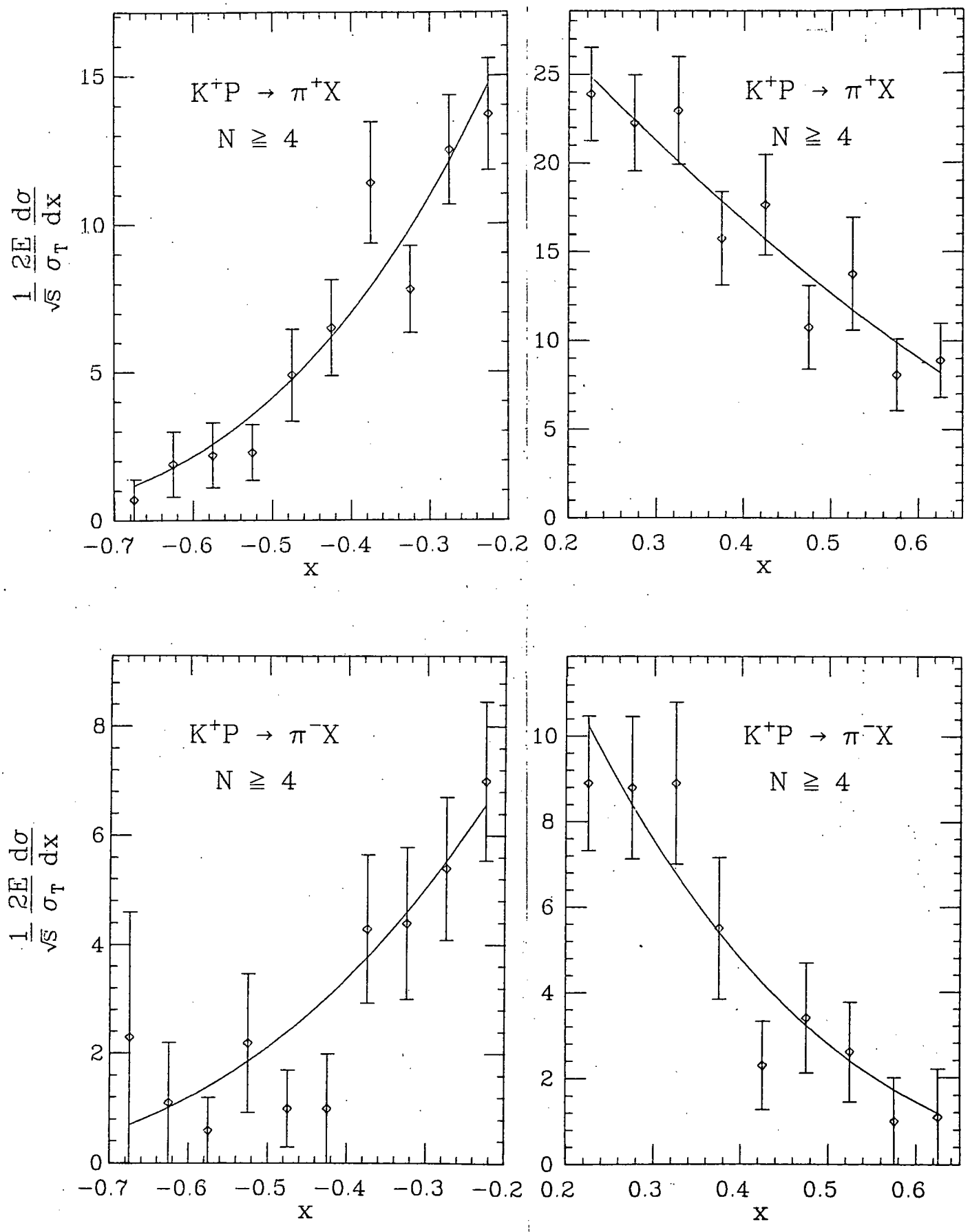
$K^+P \rightarrow \pi^+X$
$N \geqq 4$
$\frac{1}{\sqrt{s}} \frac{2E}{\sigma_T} \frac{d\sigma}{dx}$
x
$K^+P \rightarrow \pi^+X$
$N \geqq 4$
x
$K^+P \rightarrow \pi^-X$
$N \geqq 4$
$\frac{1}{\sqrt{s}} \frac{2E}{\sigma_T} \frac{d\sigma}{dx}$
x
$K^+P \rightarrow \pi^-X$
$N \geqq 4$
x

Fig. 6

The fits shown here are to spectra with 2-prong events removed, in order to reduce the diffractive component of particle production, which is excluded in the theoretical calculations. However, in the region of x covered, there is so little diffractive production, and so little 2-prong contribution, that there is very little difference for the fits done with the 2-prong events included.

The fit parameters are summarized in Table I. In this Table, the first line for each beam particle shows results for production of a pion of like charge (favored), the second line for a pion of opposite charge (unfavored). The most notable result in the $x > 0$ region is the difference in the values of the exponent n for these two cases, the exponent for the unfavored charge being higher by approximately two for each incident particle. This difference can be understood at least qualitatively in terms of a quark cascade model: $\pi^+(u\bar{d})$ and $K^+(u\bar{s})$ can both produce π^+ in the first step of a quark cascade (see Fig. 7), where the available quark energy is at the maximum. They can first produce π^- only in the second step of the cascade where the available energy is lower. Therefore, the π^- spectrum will fall more steeply with energy, and longitudinal momentum x.

Brodsky and Gunion[5] calculate the exponent n by counting the number n_s of spectator quarks at the production vertex: $n = 2n_s - 1$. Each step of the cascade produces more spectators to divide the available energy. The actual value of n_s depends on whether quark exchange or gluon exchange

TABLE I: Values of the Exponent n from Fits of $(2E/\sigma_T)(d\sigma/dx)$ to $(1-x)^n$

Reaction	$-0.7 \leq x < -0.2$	χ^2/D	$0.2 \leq x < 0.7$	χ^2/D
$K^+p \to \pi^+$	2.9 ± 0.4	8/8	1.5 ± 0.2	5/7
$K^+p \to \pi^-$	2.6 ± 0.6	5/8	3.0 ± 0.5	4/7
$\pi^+p \to \pi^+$	3.5 ± 0.4	5/8	1.0 ± 0.2	15/7
$\pi^+p \to \pi^-$	4.9 ± 0.5	4/8	2.6 ± 0.3	21/7
$\pi^-p \to \pi^-$	3.8 ± 0.4	22/8	1.1 ± 0.2	24/7
$\pi^-p \to \pi^+$	3.8 ± 0.2	5/8	2.5 ± 0.1	5/7
$pp \to \pi^+$	3.9 ± 0.2	7/8		
$pp \to \pi^-$	3.7 ± 0.3	8/8		

QUARK CASCADE DIAGRAMS

(a) Beam Vertex

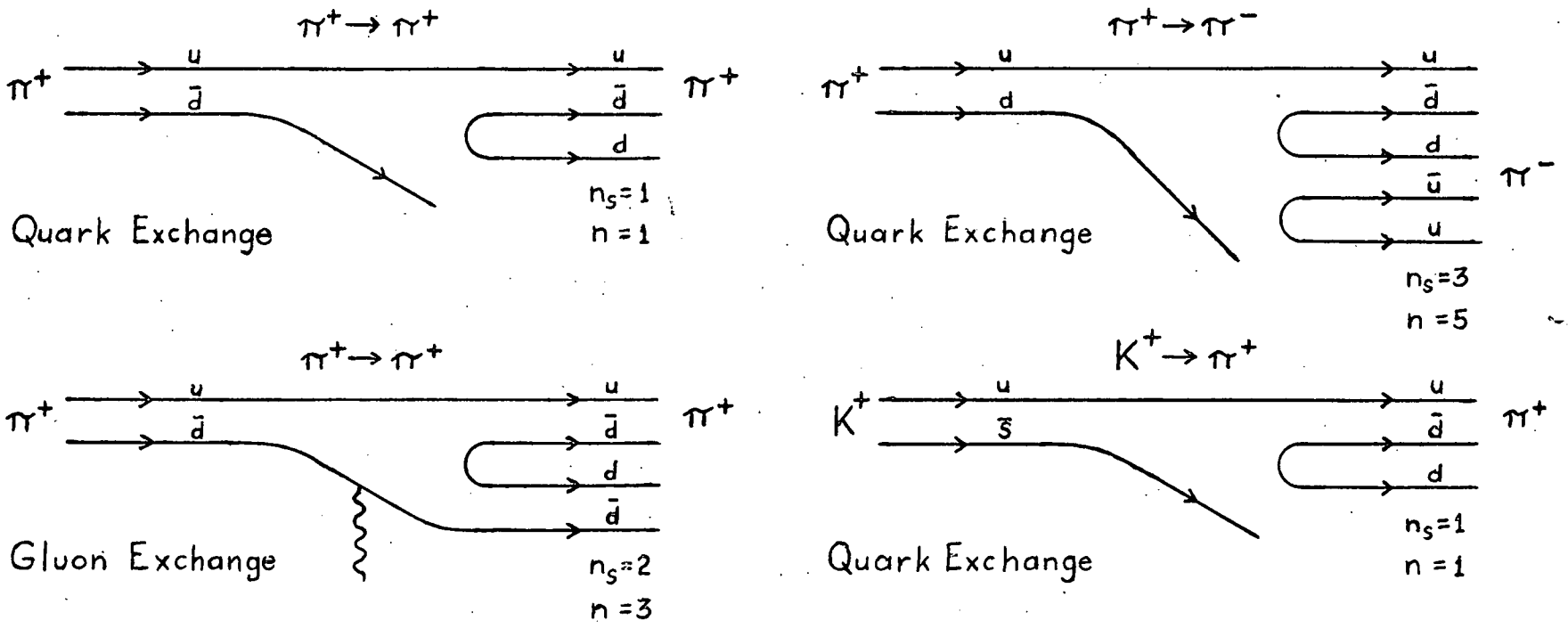

(b) Target Vertex

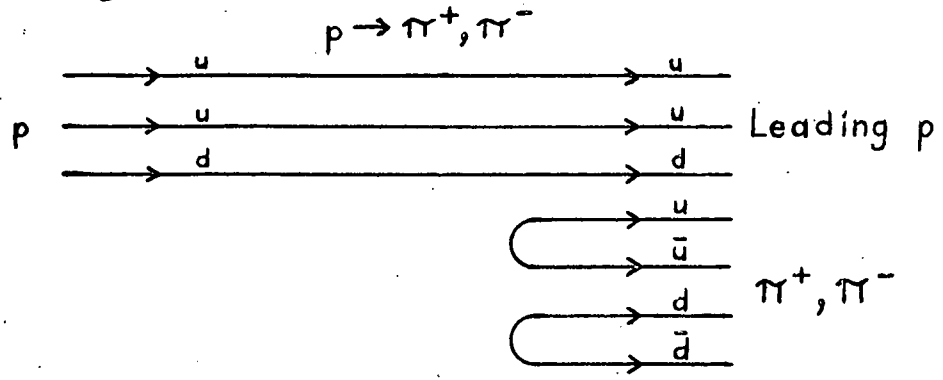

Fig. 7

is the mechanism of the overall interaction, gluon exchange producing one more spectator in each case. In Table I we see that, in the forward direction, the exponent determined for $K^+p \to \pi^+$, $\pi^+p \to \pi^+$, and $\pi^-p \to \pi^-$ agree well, within the errors, with the Brodsky-Gunion value of $n = 1$ calculated from the quark-exchange diagrams. Although the n values for K^+p are slightly higher than the others, they agree within 1 to 2 standard deviations, so no firm conclusions can be drawn about the effect of the presence of strange quarks. The value for $pp \to \pi^-$ also agrees with the Brodsky-Gunion quark-exchange $n = 3$. However, we find the unfavored reactions have $n \sim 3$, while the Brodsky-Gunion quark-exchange count would give $n = 5$. Our experimental values are in quite good agreement with other experimental determinations.[8-10]

In the backward direction, $x < 0$, we are looking at the cascade of the quarks of the target proton in each case, and have removed leading protons (identified by ionization, since these are slow in the lab). We are therefore looking at the second stage of the cascade, where π^+ and π^- are produced with equal ease (Fig. 7); the relatively high values of n, and the similarity of n in all these interactions, are consistent with the cascade picture. The absolute value of n is, however, lower than one would expect according to Brodsky and Gunion.

REFERENCES

1. A. H. Mueller, Phys. Rev. D2, 2963 (1970).
2. H. D. I. Abarbanel, Phys. Lett. 34B, 69 (1971).
3. Review: D. Horn and F. Zachariasen, Hadron Physics at High Energies (Benjamin, New York, 1973).
4. K. P. Das and R. C. Hwa, Phys. Lett. 68B, 459 (1977).
5. S. J. Brodsky and J. F. Gunion, Phys. Rev. D17, 848 (1978).
6. U. P. Sukhatme, XIIIth Rencontre de Moriond, Les Arcs, March 1978.
7. R. D. Field and R. P. Feynman, Nucl. Phys. B136, 1 (1978).
8. J. R. Johnson et al., Phys. Rev. D17, 1292 (1978).
9. J. Singh et al., Nucl. Phys. B140, 189 (1978).
10. D. Cutts et al., Phys. Rev. Letters 43, 319 (1979).

(c) The Argonne π^+p Bubble Chamber Experiment.

This experiment, studying π^+p interactions at 4.1 GeV/c in the Argonne (now FNAL) 30" chamber, is rapidly being completed. Martin Heller is in the final stages of data analysis and thesis writing. His thesis, a study of the one-constraint final state $p\pi^+\pi^0$, will be the fourth one on this experiment.

Considerable progress has been made during the past year. Various samples of the data have been studied in detail for possible biases. They have also been studied under several variations of the prism plot method of analysis. This method, which appears to be the best one available for the separation of a three-body final state into the several quasi-two-body intermediate channels producing it, is quite sensitive to the exact procedures and parameters used in the analysis. As a result of this study we are confident that our final channel separation will be a reliable one.

II. Experimental Runs in Progress and in Preparation.

(a) High Statistics Study of Particle Production and Dynamics from x = 0 to x = 1 and the Dependence on Incident Quantum Numbers (FNAL Experiment 570).

Experiment 570, which was approved in the spring of 1978, will be a comprehensive study of the dynamics of hadron production in hydrogen using five incident particles: $\pi^\pm$, K^+, p, and $\bar{p}$, all at a momentum of 200 GeV/c. We are primarily interested in the production characteristics

of particles and resonances in interactions with target protons, particularly in the central region, and in the dependence of these characteristics on the quantum numbers of the projectile particles. Such dependences may be a direct consequence of the kinematic distribution of quarks in the incident channel, and thus can give information on the structure of the interacting particles as well as on the dynamics of the collisions.

Almost all charged secondary particles produced with momenta between 5 and 50 GeV/c will be identified in the downstream CRISIS system, which takes many samples of a particle's relativistic rise in ionization. Together with particle identification, the associated drift chambers and proportional wire chambers of the hybrid system provide excellent measurements of the directions and momenta of the particles. Also, neutral particles decaying into forward-going gammas, and other particles and resonances decaying with one or more forward gammas, will have their directions and energies precisely measured by the Forward Gamma Detector. Many V^o's (Λ^o, $\bar{\Lambda}^o$, and K^o_s) will also be identified and measured in either the bubble chamber or the downstream chambers or both. Hence, for the first time in Fermilab multi-particle experiments, almost all particles produced, both charged and neutral, particularly in the central region, will be well identified and measured.

Some of the specific physics topics to be investigated are listed below and are described in somewhat more detail in the accompanying Renewal Proposal.

(i) Single-particle distributions for identified charged and neutral particles.

(ii) Multiplicity studies, in reactions of the type a + b → c + X, where a and c take on many identities in this single experiment, as well as in interactions of the type a + b → X.

(iii) Correlation studies, including the question of neutral-charged particle correlations about which little is known. Questions of local conservation of transverse momentum, strangeness and other quantum numbers will be checked in a definitive way, not possible when only charged particles are identified.

(iv) A systematic study of resonance production in the inclusive reactions:

$$\begin{pmatrix} \pi^{\pm} \\ K^{+} \\ p^{\pm} \end{pmatrix} + p \rightarrow \begin{pmatrix} \eta^{o} \\ \rho^{\pm}, \rho^{o} \\ K^{*\pm}, K^{*o} \\ \phi^{o} \\ \omega^{o} \\ \Delta^{++}, Y^{*} \end{pmatrix} + X \ .$$

Of these reactions, only those leading to ρ^{o} and Δ^{++} have been studied in any detail at Fermilab energies. The connection of resonances with clusters will be clarified.

(v) Four-constraint fits extended to events with one, two, and even three π^{o}'s and events with charged K's.

(vi) Investigation of the large amounts of forward-going neutral energy observed in our experiment E-154 in low multiplicity events.

In addition, some more spectulative areas include:

(vii) A search for a possibly new phenomenon where both projectile and target end up near $x = 0$.[1]

(viii) A search for charm and other new particles that decay into one or more heavy particles and several pions.

(ix) A study of pairs of identical heavy particles to compare with the Bose-like behavior seen in identical pion pairs.

Because of the unique capabilities of the 30" hybrid system, Fermilab has approved a 25-week run of the facility, divided between two groups of experimenters: our Consortium, now expanded to the International Proportional Hybrid System (IPHS) Consortium upon the addition of several European, Israeli, and Japanese groups, will run Experiments 570 and 565 concurrently during 15 weeks; and a collaboration of Argonne, Cambridge, Duke, Fermilab, Michigan State, and Notre Dame groups will run Experiment 597 during a ten-week period. The fifteen-week run will provide us with a minimum of 1.5 million pictures and we may obtain between two and three million pictures if no major troubles occur.

The first million pictures will be taken using a tagged positive beam of 200 GeV/c momentum, composed of approximately 10% K^+, 45% π^+, and 45% p. The next 0.5 to about one million pictures will be taken with a tagged 200 GeV/c negative beam, enriched to about 20% $\bar{p}$ and with 80% π^- and perhaps a few percent K^-. Thus we shall be able to study the topics of

interest with high statistics and will be able to make intercomparisons with minimum systematic errors. We expect that definitive, precise new data will be produced by these experiments, and that unexpected phenomena may be uncovered.

The Fermilab "contract" for Experiments 570 and 565 was signed this summer, which provides for the start of testing in January 1980 of the downstream components at FNAL and for the start of data-taking immediately after the accelerator shut-down in the fall of 1980.

(b) A Study of the Detailed Characteristics of Hadron-Nucleus Collisions Using the Fermilab Hybrid Spectrometer (Fermilab Experiment 565).

This experiment has been approved to run concurrently with E-570. We are planning to study with precision the dependence on incident particle, energy, and target of multiparticle production in hadron-nucleus collisions. Metallic foils of aluminum, silver and gold placed within the 30-inch chamber will be used as targets, and the hybrid bubble chamber spectrometer with the downstream particle identifier will be used as the detector. The thin metal foils of aluminum, silver, and gold placed in the bubble chamber for E-565 will not interfere with the other experiment, with interactions occurring in either the foils or the liquid in the chamber. For E-565 particularly, a beam of protons at 400 GeV/c or higher will be sent through the bubble chamber for a few hundred hours at the end of our run, in order to study the energy dependence.

Previous experiments[2-5] have indicated that the nucleus provides a powerful tool for the study of strong interactions, particularly for the investigation of the nature of the state of hadronic matter that exists between the instant of collision of two hadrons and the final production of particles. Many efforts have been made to interpret the general features of multiparticle production in hadron-nucleus interactions in terms of quark-parton models; at present, existing data are inadequate to distinguish among these models.[6-9]

For each incident particle and energy, the A dependence of the average multiplicity and the rapidity distributions of outgoing particles will be investigated. The hybrid system will provide 4π coverage, good spatial resolution of tracks, good momentum measurements up to the highest energy, as well as particle identification of pions, kaons and protons. The visual observation of the interaction vertex in the bubble chamber will keep systematic errors at a minimum, allowing a one-percent determination of multiplicities. This is essential for a definitive test of the models which have been developed. The hybrid spectrometer will measure the true rapidity distribution of the secondary particles, unlike other experiments which have yielded only the pseudo-rapidity.

In addition, it will be possible to detect and study the decays of associated strange particles as a function of A. This will be the first comprehensive study of this subject.

This experiment is described in more detail in the accompanying Renewal Proposal.

REFERENCES

1. M. Jacob, private communication.

2. W. Busza et al., Phys. Rev. Lett. 34, 838 (1975).

3. M. Binkley et al., Phys. Rev. Lett. 37, 571 (1976).

4. D. C. Hom et al., Phys. Rev. Lett. 37, 1374 (1976).

5. L. Kluberg et al., Phys. Rev. Lett. 38, 670 (1977).

6. B. Anderson, Proceedings of the VIIth International Colloquia on Multiparticle Reactions, Tutzing (1976).

7. A. Krzywicki, Proceedings of the Topical Meeting on Multiparticle Production from Nuclei at Very High Energies, Trieste (1976).

8. S. J. Brodsky et al., SLAC-PUB-1930 (1977).

9. A. Capella and A. Krzywicki, Phys. Lett. 67B, 84 (1977).

(c) Improvements in the Hybrid System.

The experiments just discussed above, E-565 and E-570, depend upon three major improvements to the 30-inch hybrid system: (1) larger proportional wire chambers and drift chambers have been built to provide a much wider downstream solid-angle acceptance than in the past along with a more precise determination of charged-particle trajectories; (2) the full-scale forward gamma detector has been completed and is ready for final testing; and (3) the full-sized CRISIS system for the identification of secondaries with momenta between 5 and 50 GeV/c, by means of ionization sampling, is being assembled.

Three large drift chambers and a new proportional wire chamber are now essentially completed and ready for testing. The new chambers have a sensitive area of approximately 1 m x 1 m, as compared with the 30 cm x 30 cm which we have used up to now. We shall thus have about a ten-fold increase in acceptance solid angle.

Two years ago a 1 m x 1 m x 1 m module of the CRISIS system was constructed and tested very successfully. It was then planned to construct a 2 m x 1 m x 1 m module to add to the first one in order to have a 3 m long instrument. However, a year ago it was decided to use a single 3 m x 1 m x 1 m module instead of two separate ones. The new apparatus has been built and is now being assembled.

The Brown group took on the responsibility of designing and constructing the gas system for CRISIS. The original module used pre-mixed

gases which flowed through the system and then were exhausted to the atmosphere. Since this procedure would be too wasteful for the final system, especially for a run of approximately a year's duration, a recirculating system was designed. The apparatus that was built and successfully tested includes precise control of the gas pressure throughout, precise monitoring and adjustment of the ratio of carbon dioxide to argon in the mixture, and continuous monitoring and removal of any oxygen. Anatole Shapiro spent one-half of his sabbatical year's leave at M.I.T. during the design and construction of the gas system.

All of the above improvements in the hybrid system will be installed at Fermilab by January 1980, when the final testing will begin.

(d) Charm and Vector Meson Photoproduction in a Polarized Monoenergetic Backscattered Laser Beam of 20 GeV (SLAC Experiment BC 72).

In the spring of 1979, our group joined in a proposal to study particle photoproduction using the SLAC Hybrid Facility (SHF) in a monoenergetic backscattered beam of 20 GeV photons. The topics of immediate interest include:

(1) Search for charmed mesons and baryons.

(2) Spin-dependent effects in the inclusive production of Λ's and vector mesons at large p_T and positive Feynman x, as a test of QCD predictions.

(3) Photoproduction of baryonium.

(4) A high statistics study of the production of vector mesons, especially those of higher mass such as the $\rho'(1250)$ and the $\rho'(1600)$.

Mildred Widgoff attended the July 8 EPAC meeting at SLAC at which this proposal was presented and approved, as well as the User's meeting held July 9 and 10.

An earlier proposal to move the SHF into a 20 GeV backscattered laser beam had been approved in February 1979.[1] The beam will be made by scattering laser light on a well collimated electron beam of 30 GeV/c and the backscattered light is collimated to $\sim 10^{-5}$ radians. As a result, the 20 GeV photons entering the SHF are essentially monoenergetic ($\Delta E/E = 5\%$) and polarized. We will take pictures selectively whenever we have evidence of a track emerging from the fiducial volume of the bubble chamber, but outside the $e^{\pm}$ pair area. The camera trigger is achieved with the aid of an online computer, which processes the information from the proportional wire chambers. Details of the beam and trigger are given in Reference 1.

For the photoproduction experiment, the SLAC Hybrid Facility will comprise the following elements (most of these are shown in Fig. 1):

i) 40" bubble chamber filled with hydrogen. The chamber presently operates at 15 expansions per second with a very good chance that this number can be increased to 20. The entrance vacuum window will have a thin area in the region of the pencil beam of 20 mils Al and the stainless steel entrance window will be 15 mils thick in the beam area. The downstream windows will remain unchanged. We will use 75 cm of the visible 1 meter hydrogen as fiducial volume.

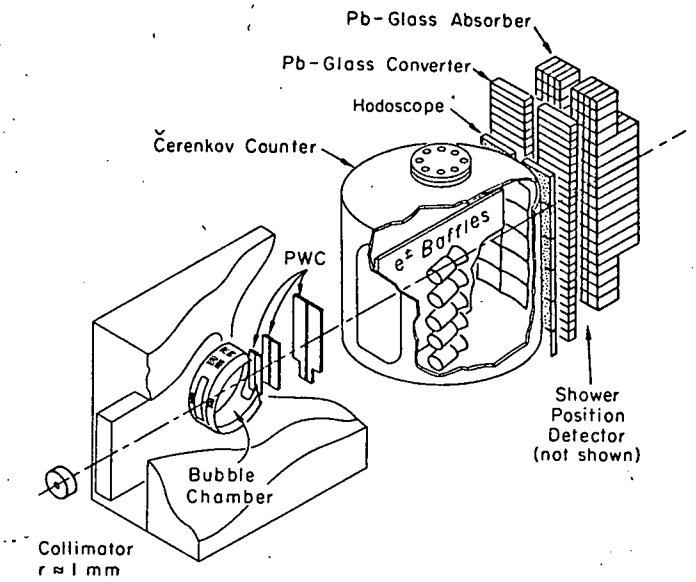
Pb-Glass Absorber
Pb-Glass Converter
Hodoscope
Čerenkov Counter
e± Baffles
PWC
Shower
Position
Detector
(not shown)
Bubble
Chamber
Collimator
r ≈ 1 mm

Fig. 1

ii) Proportional wire chamber stations (α, β, γ) in the fringe field of the 26-kilogauss magnetic field provide the hadronic trigger for the flash lamps of the bubble chamber. These chambers will be made insensitive in the $e^{\pm}$ pair area.

iii) The large aperture Cerenkov counter (CANUTE) consisting of twelve mirrors and phototubes has a radiator length of 2 meters. We plan to use Freon 12 at one atmosphere allowing $\pi/(K,p)$ separation from 3 to 10.5 GeV/c, $\pi/K/p$ separation from $\sim$10.5 to $\sim$13 GeV/c using pulse height analysis, and $(\pi,K)/p$ separation above $\sim$13 GeV/c. However, it has been proposed that the present Cerenkov counter be replaced by two large-aperture atmospheric Cerenkov counters each of twelve sections. One will contain a high index-of-refraction gas (neopentane is planned) and the other nitrogen. The new Cerenkov counters will provide $\pi/K/p$ separation over a wider momentum range. They also contain fewer radiation lengths than the present Cerenkov counter which has a thick walled pressure vessel. In addition, the total length of the two atmospheric counters is expected to be less than the present counter.

iv) Lead-glass columns provide photon detection and electron identification. The photon detector has left and right columns with adjustable space between for the $e^{\pm}$ pair area. Each column has an active converter, a position monitor, and an absorber. The information from the lead-glass columns will initially be used passively. We are considering using this information in the camera trigger provided an online algorithm can be developed that does not give an excessive trigger rate ($\leq$5% more pictures).

vi) The online NOVA-840 computer will have two 168E microprocessors connected to the CAMAC dataway. These processors will read the PWC information for each beam pulse (all photons come within 10 nsec) and determine if a track originates from the bubble chamber fiducial volume with momentum greater than 2 GeV/c. The online algorithm provides the camera trigger within the 3 msec which is normally necessary for the bubbles to grow large enough to be photographed.

Elements of the beam line are being prepared, and components of the SHF are being improved. The plan is to move the SHF into the new beam line during this fall and winter, and the bubble chamber is expected to be operational again by March 1980.

Our graduate student, Steven Kovner, worked at SLAC during the month of August on improving the trigger algorithm. He summarized his work in SLAC BC Note 55 and has expanded this for a Brown internal report (Sec. V, Reference 315).

The film from this SLAC experiment has three views of the bubble chamber all on one 70 mm film. We are now engaged in the design of a film transport and projection system to accommodate this film, and we believe that we can modify some of our present equipment to do the job. We will scan and rough-digitize the events at Brown, and then precision measure them using the PEPR system at M.I.T.

Further details of the experiment are given in our Proposal for 1980.

REFERENCES

1. J. Ballam et al., "Proposal to Move the SLAC Hybrid Facility into a 20 GeV Backscattered Laser Beam," October 1978.

(d) Comparison of Hard and Soft Hadronic Interactions in the European Hybrid Spectrometer (EHS) with a π^+/K^+p Beam at 250 GeV/c (CERN Proposal SPSC 75-18/P44 with 1978 and 1979 Updates).

Early in 1978 we joined with our colleagues at M.I.T. and Yale and with groups around Europe and Israel in proposing this experiment to be performed at CERN. This is an extension of our Fermilab experiments up to the highest energies available, using a hybrid facility that has many advantages over the one at FNAL.

The European Hybrid Spectrometer is designed to provide a unique facility for a new generation of hadron experiments. The major components are shown in Figure 1 and consist of:

1. A rapid-cycling bubble chamber (RCBC) as the 4π vertex detector, which combines both good spreading of charged-particle jets by the high magnetic field (3T) and high spatial resolution.
2. A downstream spectrometer with a strong magnet which, together with the RCBC, will provide momentum measurements of charged secondaries with errors of 1-2% over the entire range of secondary momenta.

3. An ISIS system and a silica aerogel Cerenkov detector (SAD) for charged particle identification up to 100 GeV/c. For still higher momenta a transition radiation detector is being considered.
4. Lead-glass gamma detectors for forward and intermediate angles, FGD and IGD, respectively, will provide energy measurements of the total π° component in the cms forward hemisphere. In the case of only one or two forward π°'s, their kinematic reconstruction will have the same precision as that of charged tracks.

All of these components will be completed and installed at their assigned location at CERN late in 1979, and final testing will begin. After the long shut-down early in 1980 for construction of the $\bar{p}p$ colliding facility, experiments with the EHS are scheduled to begin in the last half of 1980.

Our experiment is one of several that are approved in general, but none of these have yet been assigned specific running periods. We have requested a 20-day run producing about 4 million pictures and 930,000 events at a beam momentum of 250 GeV/c, of which 10% will be K^+ induced, 23% π^+ induced, and 67% p induced.

The physics interest in this experiment is described briefly in the accompanying Renewal Proposal. Anatole Shapiro spent three months this spring at CERN, while on sabbatical leave, studying the EHS system and learning about the software being developed for the analysis of the events.

III. Associated Matters.

In December 1978 our group ordered a new DEC PDP 11/34 minicomputer system to replace our old PDP 9 equipment, after investigating systems and bids from several other manufacturers. The PDP 11/34 arrived in May 1979 and new interfaces to our scanning and measuring machines have been designed and built. The necessary software changes have been made in the RSX-11M operating system and these are now being debugged. David Brick has directed this work.

Brown University has also upgraded the equipment at the Computer Center considerably this year. The IBM 370/138 has been replaced by a 370/148, and the very old IBM 360/67 has been replaced by a 370/158. All the important peripherals have been much improved, so that we now have excellent computing facilities.

After a long and thorough search the Department of Physics hired Dr. Hanna S. Rudnicka as an Assistant Professor of Physics to work with the hybrid bubble chamber group. She has had considerable experience in Poland working on experiments performed at CERN and Serpukhov. For the last three years she participated in Fermilab bubble chamber experiments while at the University of Washington. Hanna came to Brown on August 1, and we are all pleased with the strength which she is adding to the group and the Department.

While in Europe on sabbatical leave, Professor Shapiro was invited to participate in the XVIII Internationale Universitätswochen für Kernphysik,

at Schladming, Austria, and in the XIV Rencontre de Moriond, at Les Arc, France. At both conferences he reported on the most recent results from FNAL experiments 154 and 299. He then was invited to the European Physical Society International Conference on High Energy Physics, held in Geneva, Switzerland on June 27-July 4, in honor of the 25th anniversary of the founding of CERN.

IV. Scientific Personnel Associated with the Bubble Chamber-Hybrid System Program.

A. M. Shapiro	- -	Professor
M. Widgoff	- -	Professor
H. S. Rudnicka	- -	Assistant Professor
D. H. Brick	- -	Research Associate
D. Lewis	- -	Research Assistant
S. Kovner	- -	Graduate Research Assistant
M. Heller	- -	Graduate Student

V. Papers Published During the Preceding Year and Papers in Press.

304. D. Brick, D. Fong, M. Heller, A. M. Shapiro, M. Widgoff, and coauthors, "Inclusive Δ^{++} Production in $\pi^- p$ Interactions at 147 GeV/c," Phys. Rev. D18, 3099 (1978).

305. D. Brick, D. Fong, M. Heller, A. M. Shapiro, M. Widgoff, and coauthors, "Triple-Regge Analysis of the Reactions $\pi^- p \to p_{slow} + X$ and $\pi^- p \to \pi^-_{fast} + X$ at 147 GeV/c," Nucl. Phys. B150, 109 (1979).

306. D. Brick, A. M. Shapiro, M. Widgoff, and coauthors, "Inclusive and Semi-Inclusive Charge Structure in $\pi^- p$ Multiparticle Production at 147 GeV/c," Nucl. Phys. B152, 45 (1979).

307. D. Brick, M. Widgoff, and coauthors, "Topological Cross Sections for $K^+ p$, $\pi^+ p$, and pp Interactions at 147 GeV/c," Bull. Am. Phys. Soc. 24, 44 (1979).

308. D. Brick, M. Widgoff and coauthors, "The Four-Prong, Four-Constraint Final State in $\pi^+/K^+/p$ - p Interactions at 147 GeV/c," Bull. Am. Phys. Soc. 24, 44 (1979).

309. A. M. Shapiro and coauthors, "Comparison of Δ^{++} Production in $\pi^{\pm} p$, $K^+ p$, and pp Interactions at 147 Gev/c," Bull. Am. Phys. Soc. 24, 45 (1979).

310. A. M. Shapiro, M. Widgoff, and coauthors, "Neutral Strange Particle Production in $\pi^+/K^+/p$ Collisions on Hydrogen at 147 GeV/c," Bull. Am. Phys. Soc. 24, 45 (1979).

311. A. M. Shapiro, M. Widgoff, and coauthors, "Forward Gamma Production in $\pi^+ p$ and pp Interactions at 147 GeV/c," Bull. Am. Phys. Soc. 24, 45 (1979).

312. A. M. Shapiro and coauthors, "Comparison of Hadron Electroproduction and Hadrons Produced by π^-, π^+, K^+, and Protons on Protons," Bull. Am. Phys. Soc. 24, 636 (1979).

313. D. Brick, A. M. Shapiro, M. Widgoff, and coauthors, "Multiparticle Correlations as a Link Between Low-p_T and High-p_T Physics," Bull. Am. Phys. Soc. 24, 636 (1979).

314. M. Widgoff, D. Brick, and coauthors, "$K^+ p$ Single Particle Inclusive Production at 147 GeV/c," Bull. Am. Phys. Soc. 24, 637 (1979).

315. S. B. Kovner, "Least Squares Algorithm for Online Trigger of the SLAC Hybrid Facility," SLAC BC 72 Note 55 and Brown University High Energy Physics Internal Report #201 (Aug. 1979).

316. D. Brick, A. M. Shapiro, M. Widgoff, and coauthors, "Extraction of Off-mass-shell $\pi\pi$ and $K\pi$ Interactions," Xth International Symposium on Multiparticle Dynamics, Goa, India, Sept. 1979 (to be published).

317. D. Brick, A. M. Shapiro, M. Widgoff, and coauthors, "Inclusive Δ^{++} Production in pp, K^+p, π^+p, and π^-p Interactions at 147 GeV/c," Xth International Symposium on Multiparticle Dynamics, Goa, India, Sept. 1979 (to be published).

318. D. Brick, A. M. Shapiro, M. Widgoff, and coauthors, "High-Tranverse-Momentum Jets in 147 GeV/c π^-p Interactions," Xth International Symposium on Multiparticle Dynamics, Goa, India, Sept. 1979 (to be published).

319. D. Brick, A. M. Shapiro, M. Widgoff, and coauthors, "Comparison of 147 GeV/c π^-p Low-Tranverse-Momentum Production with Deep-Inelastic Electroproduction," Phys. Rev. Letters (1979) (in press).

320. D. Brick, A. M. Shapiro, M. Widgoff, and coauthors, "Neutral Particle Production in π^-p Interactions at 147 GeV/c and Comparison to Charged Particle Production," Phys. Rev. D (1979) (in press).

321. D. Brick, A. M. Shapiro, M. Widgoff, and coauthors, "Inclusive Production of Neutral Strange Particles by 147 GeV/c $\pi^+/K^+/p$ Interactions in Hydrogen," Phys. Rev. D (1979) (in press).

322. D. Brick, A. M. Shapiro, M. Widgoff, and coauthors, "Inclusive Δ^{++} Production in pp, K^+p, π^+p, and π^-p Interactions at 147 GeV/c," Phys. Rev. D (1979) (in press).

323. A. M. Shapiro, "Progress Report of a Research Program in Experimental High Energy Physics", October 1979.